CRITICAL REVIEW

Check for updates

Blood microfluidics: progress and challenges

Sana Sheybanikashani, [a] Jian Zhou [*bc] and Ian Papautsky [*ad]

Microfluidic technologies have significantly advanced whole blood analysis by enabling precise, rapid, and cost-effective diagnostic solutions. These platforms have made significant progress in overcoming longstanding challenges such as clogging caused by red blood cells (RBCs), white blood cells (WBCs), and platelets, as well as managing the non-Newtonian viscosity of blood, which affects flow stability and device performance. The direct processing of undiluted whole blood has enabled the isolation of rare cells such as circulating tumor cells (CTCs) with recovery rates of approaching 90%, and leukocyte depletion efficiencies of 80%. Material selection and sterilization compatibility are equally critical to ensure consistent device performance, biocompatibility, and reproducibility. This review examines recent developments in microfluidic processing of blood, and categorizes them into four preparation types: whole blood, lysed whole blood, diluted blood, and lysed diluted blood. This framework highlights the distinct biochemical and physical challenges of each type and provides a structured basis for evaluating how microfluidic strategies are optimized for specific diagnostic context. Recent advances are driving the development of AI-based flow control, rapid 3D-printed microfluidic fabrication, and integrated platforms that merge cell separation with imaging to improve diagnostic performance and access.

1. Introduction

Microfluidic devices have become essential in biomedical research due to their capacity to manage and analyze small fluid volumes with high precision.[1] These systems support rapid, cost-effective, and high-throughput analyses, which are particularly advantageous for point-of-care diagnostics and personalized medicine.[2] By integrating principles of fluid dynamics with biological assays, microfluidic platforms have significantly advanced both medical diagnostics and biological research.[2] They enable rapid testing and minimize sample volume requirements, making them highly suitable for clinical and laboratory applications.[3] The precision and operational efficiency of microfluidic technologies continue to drive the development of more accessible and accurate diagnostic assays.[4]

A wide range of microfluidic separation techniques has been developed to isolate and analyze target cells based on physical and biochemical properties, including size, shape, deformability, and surface markers. These techniques can be broadly categorized into passive, active, immunoselection-based, and hybrid approaches, each offering distinct advantages depending on the application. Inertial microfluidics (IMF) exploits inertial lift and Dean drag forces at intermediate Reynolds numbers to focus and separate cells in a continuous, label-free manner.[5,6] Deterministic lateral displacement (DLD) uses periodic arrays of micropillars to laterally displace cells above a defined size threshold.[7] Magnetic separation (MS) involves labeling target cells with magnetic nanoparticles and isolating them using an external magnetic field, enabling highly specific and efficient enrichment.[8] Acoustophoresis (AP) uses surface or bulk acoustic waves to manipulate cells based on acoustic contrast, facilitating gentle, label-free separation by size, density, or compressibility.[9,10] Magnetophoresis (MP), distinct from conventional magnetic separation, manipulates magnetically susceptible cells using field gradients without labeling, allowing continuous and contactless sorting.[11,12] Crossflow filtration (CFF) directs fluid across microfabricated membranes or weirs to remove smaller components, such as lysed cell debris or plasma proteins, enriching target.[13,14] Hydrodynamic filtration (HDF) passively separates cells by size and lateral position through flow bifurcations, eliminating the need for membranes.[15] Dielectrophoresis (DEP) applies non-uniform electric fields to move cells based on polarizability, enabling label-free discrimination of subtle electrical differences.[16] Immunoselection uses antibody-functionalized microchannel surfaces to selectively bind cells expressing specific surface markers. Often integrated with other techniques such as DEP or MP, immunoselection (IS) offers high specificity, although at lower throughput.[17,18] Collectively, these methods

[a] Department of Biomedical Engineering, University of Illinois Chicago, Chicago, IL 60607, USA. E-mail: papauts@uic.edu; Tel: +1 312 413 3800
[b] Department of Cardiovascular and Thoracic Surgery, Rush University Medical Center, Chicago, IL 60612, USA. E-mail: jian_zhou@rush.edu
[c] Department of Anatomy and Cell Biology, Rush University Medical Center, Chicago, IL 60612, USA
[d] University of Illinois Cancer Center, Chicago, IL 60612, USA

provide a versatile toolkit for processing blood samples, with the optimal approach determined by the target analyte, sample condition, and intended application.[19–22] Fig. 1 illustrates how these separation methods align with specific blood sample compositions (*i.e.*, whole blood, diluted blood, lysed blood, and lysed diluted blood), highlighting how sample preparation influences method selection based on processing needs.

Blood is a vital biofluid in clinical practice, offering valuable information for disease diagnosis, treatment, and management.[23] It contains a complex mixture of cellular and molecular components, including erythrocytes, leukocytes, platelets, plasma, and a wide array of biomolecules. Analysis of these components enables early disease detection, monitoring of progression, and evaluation of therapeutic efficacy.[24,25] Thus, blood analysis remains a cornerstone of modern clinical practice.[26–28] In this context, blood microfluidics refers to the use of microfluidic platforms for the selective separation of blood cells or circulating cellular components. It leverages microscale flow dynamics to isolate target populations from the complex matrices of whole or processed blood.
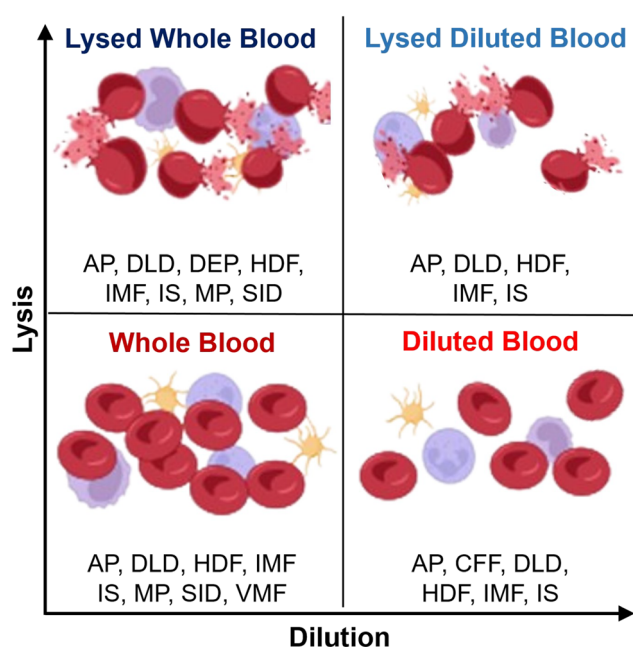
Fig. 1 Blood sample preparation techniques and their impact on cell integrity and concentration. The figure categorizes preparation methods in microfluidic systems along two axes: lysis (vertical) and dilution (horizontal). The four quadrants represent whole blood, diluted blood, lysed whole blood, and lysed diluted blood. Each quadrant lists microfluidic techniques applicable to the corresponding blood type, including acoustophoresis (AP), deterministic lateral displacement (DLD), dielectrophoresis (DEP), hydrodynamic filtration (HDF), inertial microfluidics (IMF), immunoselection (IS), magnetophoresis (MP), shear-induced diffusion (SID), viscoelastic microfluidics (VMF), and crossflow filtration (CFF). Techniques are assigned based on published literature and have been demonstrated to operate on the indicated blood type. However, many methods originally developed for whole blood can benefit from sample dilution or RBC lysis to improve separation resolution and reduce clogging.

Despite the numerous advantages, the application of microfluidics to blood analysis presents persistent technical challenges. The high cellular content and complex composition of whole blood can lead to clogging and irregular flow within microchannels, compromising device performance.[29] To mitigate these issues, sample preparation techniques such as dilution and lysis are commonly employed. Dilution modulates analyte concentrations, while lysis disrupts cellular membranes to release intracellular contents.[30] preparatory steps introduce additional complexity and potential variability, which can affect analytical accuracy and reproducibility.[31] Addressing these challenges is essential for optimizing microfluidic devices for reliable blood sample handling.[32]

This review highlights recent advancements in microfluidic technologies for the separation of cellular components from blood samples, with particular attention to associated sample preparation strategies. Prior reviews by Irimia & Toner[33] and others[34–36] have addressed general aspects of blood sample preparation, and Gomez *et al.*[37] have emphasized microfluidic approaches for blood biomarker detection. Building on these efforts, this review centers on microfluidic systems designed for cell separation. It highlight limitations of the current technologies encountered when processing whole blood and discuss emerging strategies aimed at improving the clinical utility of these platforms.

2. Blood sample preparation in microfluidics

Blood is a complex biological fluid composed of cells, proteins, nucleic acids, and metabolites, each contributing to essential physiological functions and offering valuable diagnostic information. Due to this complexity, sample preparation often involves multiple steps, including dilution, plasma separation, cell lysis, and nucleic acid extraction. While necessary, these steps are often time-consuming and can introduce risks such as sample contamination and potential exposure of laboratory personnel to pathogens. Additionally, the reagents and instrumentation needed for these processes can be costly and difficult to obtain, particularly in point-of-care or resource-limited settings.[37,38] Recent advances in microfluidics have simplified many of these sample preparation steps, making them more efficient, cost-effective, and accessible. This progress is especially impactful in remote or underserved settings, where conventional laboratory infrastructure may be lacking. Notably, microfluidic platforms have enabled the direct processing of undiluted whole blood for specific diagnostic applications, enhancing biomarker detection and expanding diagnostic capabilities. For instance, direct of whole blood analysis has been successfully applied in the detection of circulating tumor cells (CTCs) and the analysis of cell-free DNA (cfDNA).[39]

Despite these advancements, significant opportunities remain for innovation in microfluidic systems capable of processing undiluted whole blood. Eliminating the need for dilution could further simplify workflows, improve technical efficiency, and reduce overall costs.[37] Fig. 1 provides an overview

of common sample preparation techniques and their effects on red blood cells (RBCs), illustrating the combined impact of lysis and dilution. It also summarizes the microfluidic methods employed for processing blood samples. Techniques such as deterministic lateral displacement,[40,41] shear-induced diffusion,[42,43] and acoustophoresis[44–46] have demonstrated broad applicability across various blood sample types due to their effectiveness in separating cellular components. These techniques are crucial for accurate blood analysis, as they directly influence the detection and quantification of cellular elements, which is vital for both diagnostics and the investigation of disease mechanisms.[37,38]
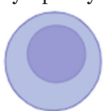
2.1. Blood composition

RBCs account for approximately 45% of the blood volume, while white blood cells (WBCs) and platelets collectively comprise about 1%. The remaining 54% is plasma, a fluid that not only suspends cellular components but also transports nutrients, oxygen, metabolic waste, and signaling molecules, including extracellular vesicles involved in intercellular communication.[37] Upon centrifugation, WBCs and platelets form a thin layer known as the buffy coat.[37] The proportion of RBCs, referred to as hematocrit, significantly influences blood rheology and can affect flow behavior within microfluidic channels of diagnostic devices. Therefore, accurate characterization of cellular components, particularly RBCs, WBCs, and platelets, is essential for the effective design and operation of such platforms.[47,48]

RBCs are primarily responsible for oxygen transport and are frequently encountered in microfluidic separation processes due to their abundance and physical properties. At higher shear rates, they deform and align with the flow, facilitating passage through narrow capillaries and ensuring efficient oxygen delivery. At lower shear rates, RBCs may aggregate, altering flow dynamics. Their deformability and interactions are thus critical for maintaining circulatory efficiency and tissue oxygenation.[49,50] Table 1 summarizes the major blood components, including

Table 1 Differences in composition between human and mouse blood

Blood cells	Human fraction (% v/v)	Human size (μm)	Human concentration/μL	Mouse fraction (% v/v)	Mouse size (μm)	Mouse concentration/μL
Red blood cells (RBCs)	~45 (ref. 83)	Disc shape: 7.5–8.7 in diameter, 1.7–2.2 in thickness[60]	Male: 4.6–6.2 million Female: 4.2–5.4 million[136]	38–45 (ref. 61)	Disc shape: 5–6 in diameter[61]	8–10 million[61]
White blood cells (WBCs)	~1 (in buffy coat)[37]		4500–11 000 (ref. 136)	~1 (ref. 137)		2000–10 000 (ref. 137)
Lymphocytes	20–40 (in WBCs)[136]	7–10 in diameter[138]	1000–4000 (ref. 136)	70–80 (in WBCs)[57]	6–9 in diameter[139]	1400–8000 (ref. 137)
Monocytes	2–8 (in WBCs)[140]	15–22 in diameter[141]	200–1000 (ref. 136)	<2 (in WBCs)[142]	12–16 in diameter[143]	<200 (ref. 137)
Neutrophils	40–60 (in WBCs)[136]	12–15 in diameter[138]	1500–8000 (ref. 136)	20–30 (in WBCs)[57]	7–10 in diameter[143]	400–3000 (ref. 137)
Basophils	<1 (in WBCs)[144]	12–15 in diameter[145]	0–200 (ref. 136)	Rare (<1 in WBCs)[57,142]	7–10 in diameter	<100 (ref. 137)
Eosinophils	0–4 (in WBCs)[136]	12–17 in diameter[146]	0–500 (ref. 136)	<7 (in WBCs)[142]	9–12 in diameter[147]	0–700 (ref. 137)
Platelets	~1 (in buffy coat)[37]	2–5 (ref. 148)	150 000–400 000 (ref. 148)	~1 (ref. 149)	1–2 (ref. 150)	200–400 000 (ref. 151)

their volume fractions and physiological functions, which are foundational for the development of microfluidic diagnostic and therapeutic systems.

Beyond its cellular complexity, blood serves as a dynamic indicator of health and disease. Routine clinical tests, such as the complete blood count (CBC), quantify these cellular components to assess physiological status.[51] Increasingly, attention has turned to rare circulating cell populations, such as CTCs, which serve as a valuable biomarker for cancer diagnosis, prognosis, and treatment monitoring.[52,53] However, the overwhelming abundance of RBCs presents a major a challenge for isolating such rare cells.[51] Reliable microfluidic enrichment demands strategies that address the high abundance of non-target cells, using approaches like size-selective filtration, immunoaffinity capture, or inertial focusing to selectively isolate rare target cells.[54,55]

Traditional blood processing methods, such as centrifugation, can lead to the loss or damage of diagnostically relevant cells.[56] As a result, there is a growing demand for separation techniques that preserve cell integrity and functionality. Microfluidic technologies offer promising solutions by enabling label-free separation based on intrinsic physical properties such as size, deformability, and density.[38] However, it is important to recognize that blood characteristics can vary significantly across species, which has implications for the translational relevance of microfluidic research.

2.2. Differences between human and animal blood

Animal models, particularly mice, are widely used in research due to their accessibility and the ability to control experimental variables. Thus, mouse blood is increasingly used in microfluidic platforms, especially given the small sample volumes (~300–500 μL) obtained per animal. As in humans, lymphocytes are the predominant leukocyte type, comprising 70–80% of the WBC differential count. These cells generally measure 6–9 μm in diameter in mice, slightly smaller than their human counterparts (7–12 μm), and possess a mildly indented central nucleus.[57] This subtle yet significant size difference may influence the performance of size-based microfluidic separation techniques, illustrating the need to account for interspecies variability during device design.[57]

Mouse neutrophils make up 20–30% of the WBC population and represent the most abundant granulocyte. In contrast, human blood is more neutrophil-rich, with neutrophils accounting for 50–70% of WBCs.[57] This difference may have functional implications, particularly in studies of immune response and inflammation.[57] Eosinophils, characterized by bright orange-red cytoplasmic granules, comprise 0–7% of murine WBCs. Monocytes, the largest leukocytes, typically represent less than 2% of the murine WBC count. Basophils are rare in mice but play roles in parasitic and allergic responses, similar to eosinophils. In humans, the leukocyte profile is skewed toward neutrophils, with lymphocytes comprising a smaller proportion (30–50%), a shift that may influence immune function and disease modeling.[57–59]

Human RBCs exhibit remarkable deformability, allowing them to traverse capillaries as narrow as 2–3 μm. These cells have a biconcave disc shape, measuring approximately 7.5–8.7 μm in diameter and 1.7–2.2 μm in thickness.[60] Hemoglobin, the oxygen-carrying protein, is housed within the RBC cytosol. RBC concentrations range from 4.6 to 6.2 million cells per μL in males and 4.2 to 5.4 million cells per μL in females. In contrast, mouse RBCs are smaller (5–6 μm in diameter) but more numerous, with concentrations of 8–10 million cells per μL.[61] The RBC membrane consists of a phospholipid bilayer supported by a spectrin-based cytoskeletal network, which confers elasticity and maintains the discocyte morphology.

Table 1 compares key differences in composition between human and mouse blood. Species-specific variations in cell size, concentration, and biophysical properties must be carefully accounted for during the design and validation of devices intended for clinical application, as these factors can substantially influence the efficiency and accuracy of cell separation processes. Overreliance on animal models may yield misleading results if human blood behavior is not adequately replicated. While animal studies are invaluable for early-stage testing, successful clinical translation requires rigorous evaluation of these differences. Furthermore, the choice of blood processing method, particularly the use of lysis, can significantly impact the accuracy and reliability of downstream analyses.

2.3. Role of lysis in blood sample analysis

Lysis, the process of disrupting cell membranes to release internal contents, is a critical step in many analytical workflows. It enables access to DNA, RNA, proteins, and metabolites for downstream applications such as flow cytometry and molecular assays. In techniques like flow cytometry and other cell-based assays, effective lysis ensures comprehensive analysis and accurate characterization of cell populations. In addition to its analytical role, lysis can be used selectively to remove specific cell types, such as RBCs, to enrich target populations prior to separation. In this review, we focus on the latter application, highlighting how lysis can enhance the efficiency and purity of target cell separation. Common lysis techniques include chemical, mechanical, osmotic, and electrical methods, each offering distinct advantages and limitations (Table 2). The choice of method depends on the specific requirements of the blood analysis, including target cell type, desired throughput, and compatibility with downstream processes.[62]

Chemical lysis uses detergents or enzymes to disrupt the cell membrane. For blood cells, saponin-based[63] and non-ionic detergents are frequently used due to their ability to lyse cells gently while preserving protein integrity.[64] For instance, RBC lysis buffer (Miltenyi Biotec, Auburn, CA) has been used to selectively lyse erythrocytes in whole blood, bone marrow, or single-cell suspensions, facilitating the recovery of leukocytes and CTCs.[65,66] This buffer works by

Table 2 Blood cell lysis methods used in microfluidic platforms

	Mechanism	Advantages	Disadvantages	Applications	Cell damage
Chemical[68,69]	Detergents or enzymes to disrupt the cell membrane	Efficient, gentle on proteins, compatible with downstream analysis	Can denature some proteins, potential contamination from lysis reagents	Suitable for lysing a variety of cells, especially for protein and nucleic acid extraction	Moderate
Mechanical[73,74,152]	Sonication, bead beating, or high-pressure homogenization to physically break cell membranes	Effective for large volumes, complete cell disruption	Causes mechanical damage to cellular components, requires specialized equipment	Ideal for applications needing complete cellular disruption, such as protein extraction from tough tissues	High
Osmotic[75,153]	Exposes cells to a hypotonic solution, causing them to swell and burst due to water influx	Simple, cost-effective	Less controlled, may cause loss of some cellular components	Suitable for applications where simplicity and cost-effectiveness are prioritized	Low
Electrical[76,154,155]	Electric field to create temporary pores in the cell membrane, allowing cellular components to escape	Highly controlled, preserves cellular organelles	Requires precise equipment, can be less efficient for large volumes	Useful for selective permeabilization, preservation of organelles, and single-cell analyses	Moderate

creating an osmotic imbalance, causing RBCs to rupture while sparing nucleated cells. It is typically diluted to a 1× working concentration and applied at a 10∶1 buffer-to-sample ratio.[65–67] Similarly, ACK lysis buffer (ammonium–chloride–potassium) to widely used to isolate WBCs from blood samples,[68–70] with protocols using a 10∶1 to 15∶1 buffer-to-sample ratio.[68,71] The buffer lyses RBCs *via* osmotic pressure, while potassium bicarbonate stabilizes pH and EDTA chelates divalent cations to prevent coagulation.[72]

Mechanical lysis physically disrupts cell membranes using external forces such as shear stress, cavitation, or friction. Techniques include sonication, bead beating, and high-pressure homogenization, which are particularly effective for processing large sample volumes or achieving complete cellular disruption.[64] For instance, Di Carlo *et al.*[73] developed a microfluidic lysis device incorporating sharp nanostructures within microchannels to enhance friction forces and penetrate cell membranes. This design increased protein accessibility by threefold compared to non-sharp filters. The device integrated sorting, lysis, and purification modules, with nanostructured filters pre-treated with bovine serum albumin (BSA) in phosphate-buffered saline (PBS) to minimize non-specific adsorption.[73] Similarly, Marshall and Tang *et al.*[74] introduced a microfluidic guillotine capable of bisecting *Stentor coeruleus* cells in a continuous-flow manner. The device operated under two regimes: low viscous stress, which induced minor membrane ruptures while maintaining high cell viability, and high viscous stress, which caused extensive rupture and reduced viability. This system achieved a throughput of 64 cells per minute, representing a >200-fold improvement over traditional methods.[74]

Osmotic lysis leverages hypotonic environments to induce water influx into cells, leading to swelling and eventual rupture of the plasma membrane. This method is simple, cost-effective, and reagent-free, but offers limited control and

may result in the loss of sensitive intracellular components. In one study,[75] osmotic lysis was integrated with inertial microfluidics to selectively lyse RBCs while preserving nucleated cells. The device continuously removed RBCs *via* exposure to deionized water, while inertial focusing concentrated nucleated cells based on size. Leukocytes were isolated with 99% separation efficiency. By modulating outlet resistance, spiked cancer cells were differentially separated with an 88% yield, while 80% of leukocytes were depleted. Importantly, the isolated cells remained viable and inactivated, making them suitable for downstream applications.[75]

Electrical lysis applies an electric field to disrupt the cell membrane, enabling the release of intracellular components. When the applied electric field exceeds a critical threshold, irreversible electroporation occurs, making this technique suitable for applications that require rapid and complete cell lysis without harsh chemical agents. This method is particularly advantageous for preserving subcellular structures such as mitochondria and nuclei, which is essential for downstream applications of organelle-specific proteomics or metabolomics. Lo and Lei[76] developed a continuous flow-through microfluidic device incorporating planar interdigitated electrodes along the bottom wall of a U-shaped microchannel. By applying an AC voltage of 20 V_{pp} at 1 MHz, they achieved complete lysis of human RBCs diluted in PBS within 7 seconds. This rapid and localized membrane disruption facilitated the release of intracellular contents into a confined flow path, enhancing the local concentration of analytes. As a result, detection sensitivity in downstream bioanalytical assays, such as immunodetection or nucleic acid amplification, is enhanced due to increased availability and accessibility of target molecules.[76]

In practice, lysis protocols are often tailored to the specific analytical objectives. For instance, in one protocol, RBC

volume fraction was quantified using a hematology analyzer followed by selective RBC lysis and fluorescent labeling of WBCs for downstream analysis.[77] In another approach, waste solutions were mixed with RBC lysis buffer, centrifuged, and resuspended for further examination.[78] Additionally, silicon-based microfilters have been used to isolate and lyse WBCs, enabling subsequent analyses such as PCR.[79,80] Standardized and optimized lysis procedures are essential for achieving reproducible results, particularly in clinical diagnostics and research settings. Effective lysis enhances assay sensitivity by releasing intracellular targets and facilitates the analysis of diverse cellular components across a range of applications.

The selection of an appropriate lysis method depends on the specific requirements of the intended analysis, including target cell type, desired throughput, and compatibility with downstream workflows. Optimizing lysis conditions is essential to minimize cell damage while preserving target analytes for accurate downstream analysis. Furthermore, the degree of blood dilution and the microfluidic environment significantly influence device performance.[81] Dilution affects flow dynamics, separation efficiency, and analytical sensitivity within microfluidic systems. Therefore, in addition to selecting an appropriate lysis strategy, precise control of dilution parameters is essential for maximizing the reliability and diagnostic utility of microfluidic platforms.

2.4. Impact of blood dilution on microfluidic processing

Dilution of blood samples for microfluidic analysis alters the relative concentrations of cellular components, such as erythrocytes, leukocytes, platelets, and plasma. This reduction in cellular density diminishes cell–cell interactions, which is critical for some separation techniques that depend on cellular dynamics, such as inertial and viscoelastic microfluidics. Dilution also alters rheological properties of blood by decreasing its viscosity and elasticity, which can disrupt flow profiles, reduce inertial focusing, and influence particle migration dynamics within microchannels.[50] Recent studies demonstrate that adjusting the dilution ratio can markedly enhance the performance of microfluidic separation systems. For example, label-free microfluidic platforms, which discriminate cells based on intrinsic physical properties (*e.g.*, size, deformability) without the use of chemical markers, can be fine-tuned through dilution adjustments to improve the isolation of rare cell types such as CTCs.[38,82]

Equally important is the understanding of cell–cell and cell–device interactions within microfluidic environments. These interactions can substantially impact diagnostic accuracy and the reliability of research outcomes. Microfluidic systems offer a unique advantage by replicating the physiological conditions of blood vessels, enabling high-resolution analysis of cellular behavior at the single-cell level.[38,82] In cancer research, for example, investigating the interactions between CTCs and other blood components provides valuable insights into metastatic processes.

Modulating blood dilution within these systems allows researchers to assess changes in both separation efficiency and intercellular dynamics, informing the development of more precise diagnostic and therapeutic approaches. Optimizing blood dilution, including dilution ratio and buffer composition, reduces cell aggregation and sample viscosity, facilitating more efficient separation and increasing the precision of downstream analyses like biomarker detection or cell counting.[83] As microfluidic technologies become increasingly integrated into clinical workflows, maintaining device sterility remains essential – particularly when processing blood samples – to prevent contamination that could compromise biological integrity and analytical validity.

2.5. Sterilization of microfluidic devices

Sterilization is essential to maintaining the safety, reliability, and functionality of microfluidic devices in both clinical and research applications. Common sterilization techniques include autoclaving, ultraviolet (UV) irradiation, alcohol treatment, and combined alcohol-UV protocols. The selection of an appropriate sterilization method is highly dependent on the materials used in the device, as different substrates exhibit varying tolerances to thermal, chemical, and photo exposure. This highlights the importance of material selection during device design – not only to ensure compatibility with sterilization protocols, but also to overcome the limitations of widely used materials such as polydimethylsiloxane (PDMS). Investigating alternative, more robust materials may enhance device durability, reproducibility, and overall performance.

2.5.1. Material selection. PDMS is a widely used material in microfluidics due to its optical transparency, elasticity, biocompatibility, and ease of fabrication.[84] However, recent studies have raised concerns regarding its long-term reliability, particularly in applications requiring electrokinetic stability and sterilization degradation. For example, Hyler *et al.*[85] reported operational failures in contactless dielectrophoresis (cDEP)-based cell sorting devices fabricated from commercially available PDMS. These failures, including bubble formation during operation, resulted in nearly 100% cell death within minutes. Despite extensive troubleshooting, the root cause was traced to undocumented changes in the PDMS formulation, underscoring the impact of batch-to-batch variability on device performance, cell viability, and reproducibility.

In addition to formulation inconsistencies, PDMS exhibits several material limitations, such as small-molecule absorption, limited solvent compatibility, and hydrophobic surface characteristics.[86] These properties complicate sterilization and reduce chemical resistance, rendering PDMS less suitable for certain applications. Consequently, alternative materials are increasingly being explored to meet the demands for enhanced chemical robustness, structural reliability, and manufacturing consistency. Thermoplastics

such as polymethyl methacrylate (PMMA), cyclic olefin copolymers (COC), polycarbonate (PC), and fluorinated polymers such as perfluoroalkoxy (Teflon PFA) and fluorinated ethylenepropylene (Teflon FEP) offer superior chemical resistance and are compatible with industrial-scale fabrication techniques such as injection molding and hot embossing. These materials can also tolerate a broader range of sterilization methods without degradation.[87] Except for PMMA, they exhibit low small molecule adsorption, making them well-suited for applications requiring high chemical stability and reproducibility. Table 3 summarizes the most commonly used sterilization methods for microfluidic devices.

2.5.2. Autoclave sterilization. Autoclaving is a widely adopted sterilization method that uses saturated steam at 121 °C and 15 psi for 15–30 minutes. It is highly effective against broad spectrum of microorganisms, including bacterial spores, and is valued for its accessibility, speed, and lack of chemical residuess.[88,89] These characteristics make autoclaving particularly suitable for applications requiring a sterile, residue-free environment. However, the high temperature and moisture involved in autoclaving can compromise the structural integrity of heat-sensitive materials and embedded electronics. Polymers commonly used in microfluidic devices may undergo warping, degradation, or delamination under these conditions. While PDMS can generally withstand autoclaving, its performance may still be affected by repeated sterilization cycles or formulation variability. Therefore, autoclaving is best suited for thermally stable materials, and alternative sterilization methods should be considered for devices incorporating heat-sensitive components. Selecting materials compatible with autoclaving not only ensures effective sterilization but also preserves device functionality and longevity.[88–90]

2.5.3. Ultraviolet (UV) sterilization. UV sterilization is an effective non-thermal method, particularly suitable for materials that are sensitive to heat. It uses UV-C light (100–280 nm) to inactivate microorganisms by inducing DNA damage. While UV sterilization is effective for surface decontamination, its limited penetration depth necessitates direct exposure of all surfaces to ensure efficacy. Since PDMS exhibits absorption to UV-C radiation, the light penetrates only a few micrometers below the surface, which significantly limits its effectiveness in sterilizing internal features that lack direct optical access.[86] Typical protocols involve exposure times of approximately 2 hours at ambient temperature.[89] This method is compatible with most materials used in microfluidic devices, although prolonged UV exposure can

degrade UV-sensitive polymers, such as PMMA and PC.[91] Therefore, material selection and device geometry must be carefully considered, especially for applications requiring repeated sterilization cycles. UV sterilization leaves no chemical residues, making it advantageous for applications demanding high purity. However, the requirement for specialized equipment and extended processing times may limit its practicality in high-throughput settings.[89,92]

2.5.4. Alcohol sterilization. Alcohol-based sterilization is widely used for surface disinfection in laboratory environments. Alcohols such as ethanol or isopropanol (isopropyl alcohol) are typically applied by soaking devices for 15–60 min at ambient temperature. Alcohol is effective against a broad range of microorganisms but exhibits limited efficacy against bacterial spores. This method is compatible with many plastics and elastomers commonly used in microfluidic devices. However, alcohol can leave residues that may interfere with downstream biological assays or compromise cell viability. To mitigate this, thorough rinsing with sterile balanced salt solutions is recommended, as demonstrated by Walker et al.[93] Despite its limitations, alcohol sterilization remains a low-cost, rapid, and accessible method, particularly suitable for single-use or low-risk applications.[89,92–94]

2.5.5. Alcohol/UV combination. The combined use of alcohol and UV light offers a synergistic sterilization strategy that enhances microbial inactivation while minimizing processing time. This method typically involves sequential exposure to alcohol and UV-C light for 10–30 min at ambient temperature, providing a balance between rapid sterilization and broad-spectrum efficacy.[89,95] The alcohol/UV combination is compatible with a wide range of materials commonly used in microfluidic devices and is particularly effective for surface sterilization. It leaves minimal chemical residues, reducing the risk of interference with downstream biological assays. While the method requires access to both alcohol and UV equipment—resulting in moderate operational costs—it is well-suited for applications demanding high sterility and material compatibility.[89,95] Importantly, the choice of sterilization strategy should also consider the biological load introduced by the sample type. For example, processing diluted blood, lysed blood, or whole blood introduces varying levels of organic material and microbial contamination, which may influence sterilization efficacy and material performance. Therefore, tailoring the sterilization protocol to both the device material and the sample type is essential for ensuring reliable and reproducible outcomes.

Table 3 Sterilization methods used with microfluidic devices

| Method	Efficacy	Time	Temperature	Material compatibility	Residue	Cost
Autoclave[88–90]	High	15 min	121 °C	Limited (heat/moisture)	No	High
UV[89,92]	Moderate to high	2 h	Ambient	Good (except UV-sensitive materials)	No	Moderate
Alcohol[66–68]	Moderate	15–60 min	Ambient	Good (some plastics/elastomers)	Yes	Low
Alcohol/UV[89,95]	High	10–30 min	Ambient	Good	Yes	Moderate

3. Diluted blood in microfluidic devices

Microfluidic devices designed for processing diluted blood are among the most commonly used.[96,97] Blood dilution – typically at a 1:10 ratio – reduces the risk of clogging and promotes stable flow dynamics, which are critical for achieving reliable cell separation and analysis. To preserve cellular integrity and maintain physiological conditions, isotonic solutions such as PBS are commonly used for dilution.[98–100]

3.1. Passive techniques

In the passive approach, microfluidic systems operate without external actuators, fields, or power sources, relying instead on intrinsic hydrodynamic forces and channel geometries to manipulate cells. Mach and Di Carlo[101] introduced a continuous scalable blood filtration device using inertial microfluidics to process large sample volumes. The system uses parallel microchannels to separate pathogenic bacteria from diluted blood based on size.[101] Fig. 2A shows a high-speed brightfield image of RBCs at equilibrium positions within 20 μm wide channel at 200 mL min^{-1}. The histogram illustrates the frequency of RBC positions within the channel width as downstream length increases. Experimental and theoretical comparisons of RBC and bead positions in expansion channels demonstrated separation efficiency. The device achieved over 80% bacterial
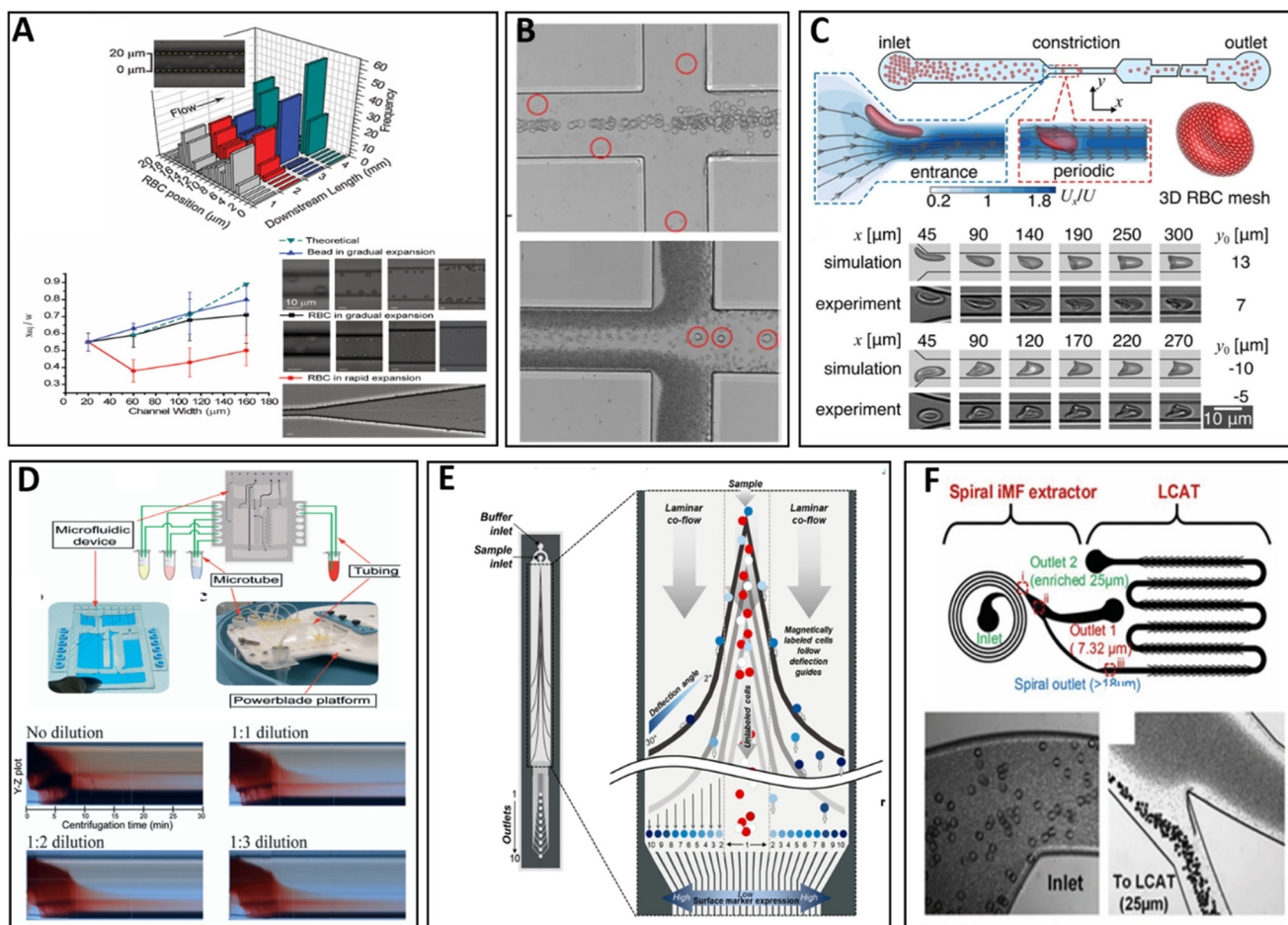
Fig. 2 Microfluidic processing of diluted blood. (A) Continuous scalable blood filtration device. High-speed brightfield image of RBCs in equilibrium positions within a 20 μm channel width at 200 μL min^{-1}, and histogram illustrating frequency of RBC positions within the channel width as downstream length increases. Reproduced from ref. 101 with permission from John Wiley and Sons, Copyright 2010. (B) Brightfield image illustrating separation of smaller cells near the channel walls and larger cells exiting through the center channel. Reproduced from ref. 102 under the terms of a CC BY-NC, Copyright 2023. (C) Measurement of RBC shear modulus. Schematic of the microfluidic chip design with a 3D mesh model of an RBC with comparison of simulated and experimental images showing RBC deformation at various positions along the microchannel. Reproduced from ref. 103 with permission from the Royal Society of Chemistry. (D) Schematic of the automated centrifugal microfluidic platform setup. Time-series images of blood fractionation using the ATPS system with varying dilutions of blood, showing distinct layering during centrifugation. Reproduced from ref. 104 with permission from the Royal Society of Chemistry. (E) Schematic of the co-based ribbon prismatic deflection chip used in the Prism Chip, illustrating how magnetically labeled cells are guided along the deflection paths based on their magnetic properties, achieving high-resolution separation of CTCs and clusters. Reproduced from ref. 105 with permission from the American Chemical Society. (F) High-throughput size-selective enrichment of cell populations. Schematic of the integrated spiral inertial microfluidics and lateral cavity acoustic transducer (LCAT) device. Brightfield images showing cell separation efficiency. Reproduced from ref. 106 with permission from the Royal Society of Chemistry.

removal after two stages, highlighting its potential for high-throughput clinical diagnostics.

Macaraniag et al.[102] developed an inertial microfluidic device to isolate CTCs from small volumes of mouse blood, addressing a key limitation in preclinical cancer models.[102] The device separates cells based on size, directing smaller cells to side channels and larger cells, such as CTCs, to a central outlet, as illustrated in Fig. 2B. Using EO771 and Py230 murine cell lines, which are notably smaller than human-derived cancer cells, the study demonstrated successful spike recovery at rates of 69–72%, confirming the device's effectiveness in isolating target cells from complex blood samples. In addition to isolation, the study evaluated the complete workflow, including cytocentrifugation and immunostaining, and emphasized the importance of assessing not only isolation efficiency but also post-processing steps that influence final cell yield and morphological integrity. This work demonstrates the utility of inertial microfluidics for CTC enumeration in murine models and highlights critical considerations for downstream analysis in translational cancer research.

Another passive method was demonstrated by Saadat et al.[103] developed a microfluidic platform to quantify RBC deformability by measuring their shear modulus, a key mechanical property that governs the ability of RBCs to traverse narrow capillaries and maintain efficient microvascular flow. This property is a clinically relevant biomarker in conditions such as diabetes, sepsis, metabolic syndrome, and neurodegenerative disorders, where pathological alterations—such as increased membrane stiffness or elevated cytoplasmic viscosity—impair cellular deformability and compromise tissue oxygenation. In their system, illustrated in Fig. 2C, RBCs flow through a 7×7 μm square microchannel, deforming into a parachute-like shape under applied shear.[103] The degree of deformation is modulated by the imposed shear rate and intrinsic cellular parameters, including membrane elasticity and cytoplasmic viscosity. As the shear rate increases, the capillary number (Ca), which represents the ratio of viscous to elastic forces, also increases, leading to more pronounced deformation, unless counteracted by pathological stiffening. The cytoplasmic viscosity ratio (λ), though constant for a given cell–medium system, influences internal flow resistance and thus affects deformation magnitude. By systematically varying shear rate, the platform captures how these parameters interact to shape RBC deformation profiles, enabling detection of subtle mechanical abnormalities. This shear-dependent behavior has direct clinical implications, as reduced deformability under physiological flow conditions is associated with microvascular dysfunction and disease progression. The integration of high-speed imaging, single-cell tracking, and computational modeling allows for real-time biomechanical phenotyping, with simulations validating experimental observations and supporting high-throughput, quantitative assessment of RBC mechanical properties.

3.2. Active techniques

Active microfluidic techniques use external energy sources, such as electric, magnetic, or acoustic fields, to manipulate fluids and cells within devices. This approach enables more complex and precise control over fluid flow and particle separation, making it especially valuable in applications such as cell sorting and diagnostics. Moon et al.[104] demonstrated a centrifugal microfluidic platform integrated with an aqueous two-phase system (ATPS) for automated fractionation and isolation of components from human blood, achieving precise and reproducible separation of RBCs and plasma. A mixture of polyethylene glycol (PEG) and dextran (DEX) served as the two-phase density gradient medium, enabling fractionation of blood samples into distinct layers.[104] As illustrated in Fig. 2D, the device design facilitated the introduction of blood samples and their separation into discrete cellular fractions, with time-series imaging confirming consistent layer formation across varying dilution levels. The platform achieved high recovery efficiency and purity, with clearly distinguishable phase boundaries and minimal cross-contamination. Quantitative assessment of reproducibility showed low variability in layer lengths, with coefficients of variation of 1.09% for the whole sample, 4.35% for plasma, and 9.72% for the RBC layer. Furthermore, post-separation cell viability exceeded 90%, underscoring the method's suitability for downstream applications requiring intact and functional cells. These results validate the platform's capability for high-fidelity blood component separation and highlight its potential utility in clinical and research workflows requiring standardized, automated sample processing.

3.3. Immunoselection techniques

Immunoselection techniques rely on the specific binding of antibodies to cell surface markers, enabling the selective capture and enrichment of target cells from complex biological samples. These methods are particularly useful for isolating rare cell populations with high specificity. Aldridge et al.[105] developed the Prism Chip, an immunomagnetic profiling and separation device for isolating live tumor cells and cell clusters from diluted blood. This chip uses prismatic deflection to separate cells based on surface protein expression, achieving a 5.7 log depletion of WBCs. Magnetically labeled cells are directed through angled ferromagnetic guides, which deflect them into distinct streams according to magnetic loading. This enables high-purity isolation of phenotypically diverse CTC subpopulations, including clusters, without compromising viability.[105] The Prism Chip's design, detailed in Fig. 2E, incorporates cobalt-based ribbon deflection guides angled between 2° and 30°, balancing magnetic and fluidic drag forces to sort cells by magnetic properties. This non-destructive method preserves cell viability for downstream functional assays and biochemical analyses. The Prism Chip addresses a critical challenge in cancer research by enabling high-resolution separation and profiling of viable CTCs, supporting liquid biopsy development and metastatic disease monitoring.[105]

3.4. Hybrid techniques

Hybrid microfluidic techniques integrate passive and active mechanisms to combine the advantages of both approaches —offering high throughput, selectivity, and flexibility in cell manipulation and separation. For example, Nivedita et al.[106] developed an integrated platform combining spiral IMF with a lateral cavity acoustic transducer (LCAT) to enable selective, on-demand cell separation. Fig. 2F illustrates the integrated device. The spiral IMF component separates cells by size, directing smaller particles to one outlet and larger particles to the LCAT section, where they are trapped in acoustic microvortices. Brightfield imaging confirmed efficient separation, with 7.32 μm particles eluting through outlet 1 and particles >18 μm retained in the LCAT region. This hybrid platform achieved over 90% depletion of smaller cells and up to 44 000× enrichment of target populations within 5 min, demonstrating strong potential for rare cell isolation and liquid biopsy applications.

The studies reviewed here highlight significant progress in using microfluidic platforms for processing diluted blood samples. Passive systems have demonstrated high-throughput capabilities for cell separation and mechanical phenotyping, while active and immunoselection-based techniques offer enhanced specificity and control for isolating rare cell populations such as CTCs. Hybrid approaches further expand the functional scope of microfluidics by integrating the strengths of both passive and active modalities. Together, these advancements highlight how microfluidic technologies are helping to tackle key challenges in both research and clinical settings. However, challenges remain, including limited throughput in some hybrid systems, reliance on labeling in immunoselection platforms, and sample dilution constraints that affect downstream analysis. Addressing these limitations through improved device integration, label-free detection strategies, and on-chip sample concentration will be critical for translating microfluidic blood analysis into scalable, real-world applications.

4. Microfluidic devices using lysed and diluted blood

The use of lysed and diluted blood samples in microfluidic systems has enabled significant advancements in the isolation, purification, and analysis of cellular and molecular components. This approach is particularly valuable for applications requiring access to intracellular contents, such as nucleic acids and proteins. Although RBCs are the most abundant cells in blood, they are rarely the focus of analysis and often interfere with the detection of rarer cell types due to strong cell–cell interactions (see section 2.3). By lysing RBCs on-chip, microfluidic platforms can reduce sample complexity and enhance the sensitivity of downstream assays, such as malaria detection and prophylactic drug analysis.[62,107] Additionally, these systems have been applied in diverse contexts, including cancer diagnostics, sepsis

detection, and single-cell analysis.[108] While microfluidic strategies are generally categorized as passive, active, immuno-based, or hybrid, devices designed for lysed and diluted blood samples fall primarily within the passive and active categories.

4.1. Passive techniques

Zhou et al.[68] developed a multi-flow microfluidic device for isolating CTCs from lysed and diluted blood samples of patients diagnosed with non-small-cell lung cancer (NSCLC). The device uses size-dependent inertial migration to separate larger CTCs from smaller WBCs, which remain near the sidewalls while CTCs migrate toward the central flow. In this system, RBCs are first lysed and WBCs suspended in buffer, eliminating interference from erythrocytes and enhancing the resolution of size-based separation. The device's inlet and outlet configuration establishes distinct flow streams, enabling precise collection of target cells. As shown in Fig. 3A(i), fluorescent imaging illustrates the influence of flow rate ratios (Q_s/Q_b) on separation efficiency, confirming effective flow control and optimal cell migration. Fig. 3A(ii) further demonstrates the device's performance, with brightfield images showing clear separation of larger particles from WBCs in spiked suspensions before and after microchannel passage. Although the method introduces additional steps—RBC lysis and dilution—that can increase complexity and risk of cell loss, it successfully isolates viable and intact CTCs with over 87% separation purity and more than 93% recovery. CTCs were detected in 75% of NSCLC patient samples, with no false positives observed in healthy controls. These results highlight the platform's potential for improving liquid biopsy workflows and advancing personalized cancer diagnostics by enabling downstream molecular and phenotypic analysis of CTCs.

Ramachandraiah et al.[75] developed an integrated microfluidic platform that combines selective RBC lysis with inertial microfluidics to achieve high-throughput separation of nucleated cells from whole blood. This approach addresses key challenges in leukocyte analysis and CTC isolation by leveraging a two-step process of hypotonic lysis of RBCs using ultrapure Milli-Q (MQ) water, followed by inertial focusing in a spiral microchannel. Exposure to MQ water induces osmotic swelling in nucleated cells while lysing RBCs, thereby enhancing size-based separation efficiency within the spiral channel. The device achieved 88% recovery of spiked cancer cells and 80% depletion of leukocytes, demonstrating its effectiveness in isolating target cells from lysed blood samples. Fig. 3B(i) illustrates the device layout and operational sequence, beginning with RBC lysis and followed by inertial focusing. Fig. 3B(ii) shows representative images of cancer cells before and after exposure to MQ water, highlighting the swelling effect that increases cell size and facilities differential migration.[75] This platform exemplifies a significant advancement in label-free, high-throughput cell separation, offering the ability to isolate viable and intact nucleated cells suitable for downstream
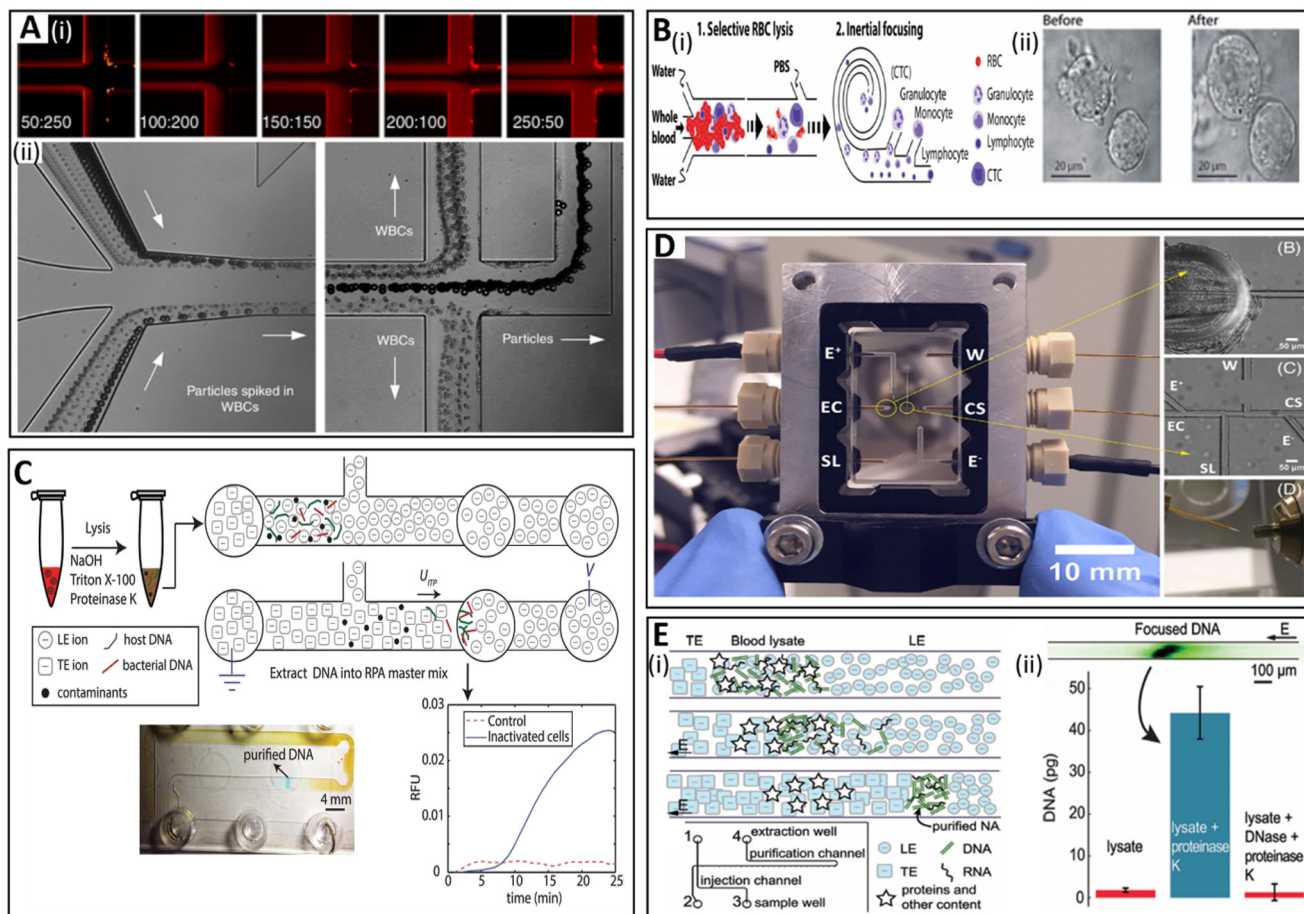
Fig. 3 Microfluidic processing of lysed and diluted blood. (A) (i) Fluorescent images of sample and buffer streams at various flow rate ratios (Q_s/Q_b), showing effective flow control for isolating CTCs from lysed diluted blood. (ii) Brightfield images displaying separation of particles spiked in WBC suspensions, demonstrating the device's capability to isolate CTCs from lysed diluted blood. Reproduced from ref. 68 under CC BY 4.0, Copyright 2019. (B) (i) Schematic of the device for selective lysis of RBCs and inertial separation of nucleated cells. (ii) Images showing cell swelling in response to hypotonic solution (MQ water). Reproduced from ref. 75 with permission from the Royal Society of Chemistry. (C) Schematic of the ITP-RPA assay protocol. It outlines the process of lysing whole blood spiked with *listeria monocytogenes* using NaOH, Triton X-100, and proteinase K, followed by ITP purification and RPA detection. Total process time is under 50 minutes, plus 25 minutes for RPA detection. Reproduced from ref. 109 with permission from the Royal Society of Chemistry. (D) Assembled microfluidic device with fluidic and electrical connections, showing the design for efficient handling and processing of blood samples. Reproduced from ref. 110 with permission from John Wiley and Sons, Copyright 2022. (E) (i) Schematic of the ITP-based nucleic acid purification process. (ii) Bar graph showing mass of nucleic acids purified from lysate treated with proteinase K, with images of the focused DNA zone within the ITP channel. Reproduced from ref. 111 with permission from the American Chemical Society, copyright 2009.

applications such as functional assays and molecular profiling. Its integration of selective lysis and inertial microfluidics enhances diagnostic and prognostic capabilities, particularly in cancer and immune monitoring. Future refinements may focus on improving separation resolution and adapting the system for broader clinical use.[75]

4.2. Active techniques

Eid and Santiago[109] introduced a method for detecting *Listeria monocytogenes* cells in whole blood by integrating isotachophoresis (ITP) and recombinase polymerase amplification (RPA). The system performs on-chip lysis, DNA extraction, and purification using ITP, followed by isothermal amplification, all within 75 min. The process begins with

chemical lysis of whole blood samples spiked with *L. monocytogenes* using a reagent mixture of NaOH, Triton X-100, and proteinase K. This lysis protocol is optimized to ensure compatibility with ITP, which employs an applied electric field to selectively extract and concentrate bacterial DNA while excluding blood-derived inhibitors. The ITP purification step, lasting approximately 40 min, is followed by direct transfer of the purified DNA into an RPA master mix for isothermal amplification and detection. This integrated approach enables sensitive and specific detection of bacterial DNA in complex biological matrices, overcoming the inhibitory effects commonly associated with PCR-based methods.[109]

The ITP-RPA assay workflow is illustrated in Fig. 3C, which outlines the sequential steps of lysis, purification, and detection. The schematic highlights the loading of lysed

blood into the microfluidic chip, the application of an electric field to initiate ITP, and the formation of a focused zone containing purified nucleic acids. This zone is subsequently transferred into the RPA reaction chamber for amplification. The integration of ITP with RPA addresses a critical need in infectious disease diagnostics by enabling rapid, reliable detection of bacterial pathogens directly from whole blood. Compared to conventional blood culture and PCR workflows, this method significantly reduces processing time and enhances analytical sensitivity, making it well-suited for point-of-care applications. The platform's ability to deliver accurate results within one hour represents a substantial advancement in the timely diagnosis and management of bloodstream infections.[109]

Václavek and Foret[110] developed a microfluidic platform that integrates single-cell extraction with electrical lysis for high-sensitivity mass spectrometry (MS) analysis of intracellular compounds. This system enables detailed biochemical profiling at the single-cell level, offering insights into cellular heterogeneity and metabolic states. The platform was demonstrated using RBCs isolated from human blood, which were subjected to a combination of high-voltage (HV) pulsing and chemical lysis to release intracellular contents. The lysis protocol involved washing RBCs with PBS–EDTA, followed by treatment with a solution containing 100 mM acetic acid, 10% isopropanol, and 10% acetonitrile. Cells were then introduced into the microfluidic chip, where electroporation and osmotic shock facilitated on-demand lysis. The resulting lysates were directed to an emitter capillary for nanoelectrospray ionization-MS (nESI-MS) analysis.

The assembled device, shown in Fig. 3D, incorporates both fluidic and electrical components, including electrodes, spray liquid and cell suspension inlets, and a flow-filtering junction that guides lysates toward the MS interface. A 100 μm neck separates the spray liquid and cell suspension streams, ensuring selective delivery of lysed material to the emitter. The emitter tip, positioned approximately 2 mm from the MS inlet, enables stable and reproducible ionization. Using this setup, the authors successfully detected hemoglobin alpha and beta chains from individual RBCs, achieving a detection sensitivity of approximately 300 amol per cell. Minimal background signal in blank controls confirmed the system's specificity and analytical robustness. Although the study did not identify additional intracellular analytes, the platform's ability to generate high-quality mass spectra from single cells highlights its potential for applications in single-cell diagnostics, drug response profiling, and metabolic analysis.[110]

Persat et al.[111] developed a microfluidic platform for purifying nucleic acids (NAs) from whole blood using ITP, offering a streamlined alternative to conventional solid-phase extraction methods. This system enables efficient lysis, extraction, and purification of genomic DNA by exploiting the electrophoretic mobility differences between NAs and blood-derived contaminants. The process begins with chemical lysis of diluted blood using a buffer containing Triton X-100, Tris-

HCl, and proteinase K, which effectively disrupts RBCs and degrades proteins.[111] The lysate is then introduced into a microfluidic chip, where an electric field is applied to focus nucleic acids into a narrow zone between a leading electrolyte (LE) and a trailing electrolyte (TE). This focused zone excludes PCR inhibitors such as hemoglobin and denatured proteins, resulting in highly purified DNA suitable for downstream amplification.

The ITP-based purification process is illustrated in Fig. 3E(i), which shows the injection of lysate between the LE and TE, the application of an electric field, and the formation of a concentrated NA zone within the microchannel. Experimental validation in Fig. 3E(ii) demonstrates a significant increase in DNA yield when lysates are treated with proteinase K, with the system recovering 44 ± 6 pg of DNA from just 2.5 nL of whole blood. This corresponds to a recovery efficiency of 30–70%, depending on the initial cell count. Real-time PCR confirmed the compatibility of ITP-purified DNA with downstream analysis, yielding consistent amplification (Ct = 30.9 ± 0.4), whereas unpurified lysates failed to amplify. The successful detection of a 201 bp BRCA2 gene fragment and matching melting temperatures between purified samples and controls further validated the method's analytical performance. This platform addresses key limitations in nucleic acid analysis from complex biological matrices, offering a rapid, high-purity, and inhibitor-free preparation method that enhances the reliability and sensitivity of genomic assays.[111]

While microfluidic systems using lysed and diluted blood have significantly advanced the isolation and analysis of cellular and molecular components, several limitations remain, including complex workflows, reliance on external instrumentation, and challenges in processing undiluted whole blood. Recent innovations have begun to address these challenges by introducing more integrated, scalable, and user-friendly platforms. For example, Ayers et al.[112] developed the PRECISE device, which combines plasma separation and NA extraction into a single, electricity-free unit, streamlining sample preparation for point-of-care diagnostics. Similarly, Hatami et al.[113] introduced a fully automated centrifugal microfluidic system capable of high-throughput isolation of cell-free fetal DNA, reducing manual intervention and improving scalability. These advancements represent important progress toward the development of next-generation microfluidic platforms that are not only efficient and robust but also accessible for decentralized and clinical use.

5. Lysed whole blood devices

Traditional blood analysis methods often rely on lysed diluted blood to facilitate precise cell sorting and analysis, primarily due to the high density and complexity of whole blood. RBC lysis reduces sample viscosity and improves accessibility of target cells such as WBCs and CTCs.[114,115] While dilution can produce similar outcomes, it adds extra steps and introduces variability, which may reduce

throughput and complicate workflows. To overcome these limitations, recent innovations have focused on using lysed whole blood directly, that is, undiluted blood in which RBCs are selectively lysed while preserving WBCs and other circulating cells. This approach combines the benefits of RBC lysis with the operational simplicity of undiluted sample processing. These approaches leverage advanced microfluidic architectures and inertial focusing techniques to streamline cell isolation and analysis, maintaining high purity and viability while minimizing processing time and complexity.[114,115]

5.1. Passive techniques

Lim *et al.*[66] explored the inertial focusing behavior of various particles, including polystyrene beads, WBCs, and PC-3 prostate cancer cells, in both physiological saline and whole blood using particle trajectory analysis (PTA). The microchannel design, shown in Fig. 4A, featured a 2 : 1 aspect ratio, promoting inertial focusing at two lateral equilibrium positions. Advanced imaging techniques enabled clear visualization of individual particles,

even at high flow velocities.[66] However, the high abundance of RBCs in whole blood introduces optical interference, limiting the effectiveness of conventional imaging methods such as high-speed brightfield and long-exposure fluorescence imaging. To address this, RBCs were lysed to isolate WBCs and better control hematocrit, thereby improving visualization and particle tracking. PTA allowed precise identification of in-focus particles at flow velocities up to 1.85 m s^{-1}.[66] This study identified a unique inertial focusing mode for PC-3 cells in undiluted whole blood (45% HCT) that was not observed in saline or diluted samples. These findings illustrate the value of RBC lysis and PTA in elucidating particle dynamics in complex biological fluids.

Zhu *et al.*[69] developed an inertial microfluidic cube, a compact inertial microfluidic device that integrates lysis, storage, and extraction modules for the automated isolation of WBCs from lysed whole blood. As illustrated in Fig. 4B, the device features three inlets for blood, lysing buffer, and PBS, and two outlets for collecting WBCs and lysed RBC debris. Whole blood is mixed with ACK lysing buffer to selectively lyse RBCs, and the resulting WBC-rich sample is extracted with high purity. The system achieved a lysis mixing efficiency of 94.2%, a
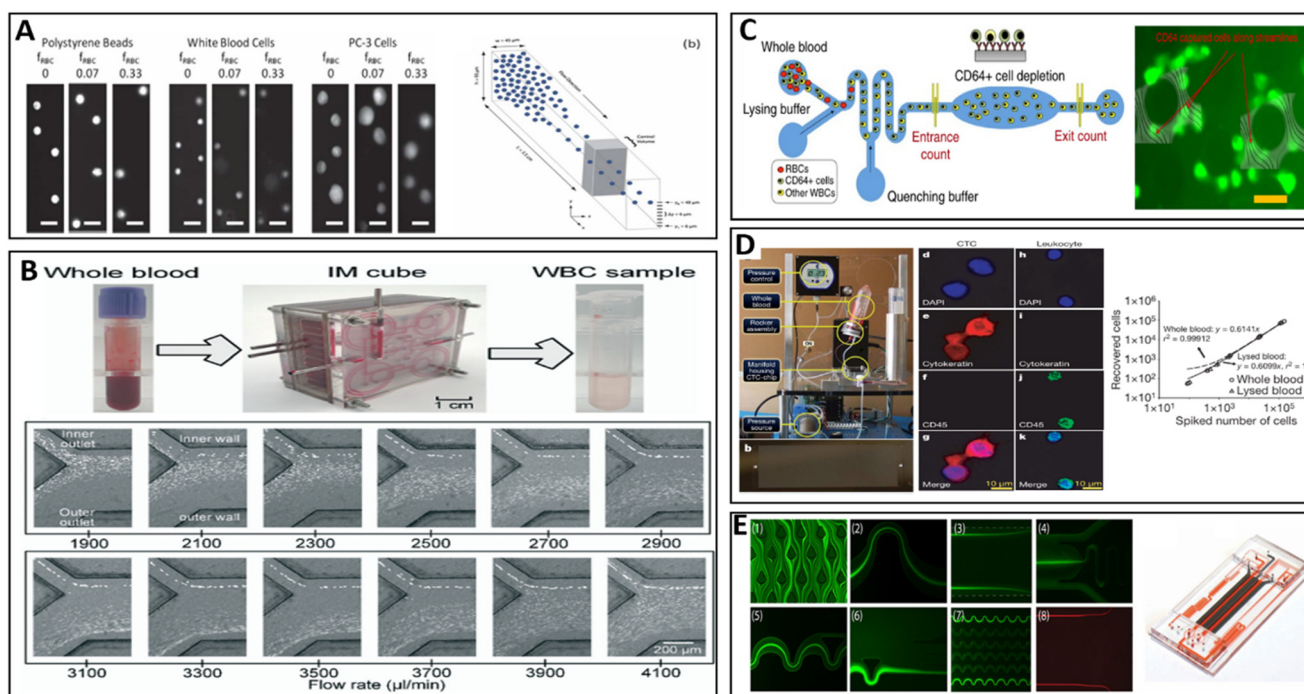
Fig. 4 Use of lysed whole blood in microfluidics. (A) Particle focusing in a straight microchannel with a 2 : 1 aspect ratio at a flow rate of 450 μL min^{-1}. Individual in-focus particles can be identified in starting samples with higher RBC volume fractions (fRBC) without significant degradation in fluorescence signal quality. Reproduced from ref. 66 with permission from the Royal Society of Chemistry. (B) The WBC sample extracted by the IMF cube. Images illustrate the distributions of 10 μm and 4 μm particles at different flow rates. Reproduced from ref. 69 with permission from the Royal Society of Chemistry. (C) Schematic of the differential expression-based cell-counting technology. Whole blood (10 μL) is infused into the biochip along with lysing and quenching buffers to preferentially lyse erythrocytes (scale bar: 40 μm). Reproduced from ref. 63 under a CC BY 4.0, Copyright 2017. (D) Workstation setup for CTC separation. The CTC-chip with microposts etched in silicon. Regression analysis of capture efficiency for various target cell concentrations, comparing whole blood to lysed blood samples. The plot represents the number of cells spiked *versus* the number of cells recovered. Merged images identify CTCs and hematologic cells. Reproduced from ref. 116 with permission from Springer Nature. Copyright 2007. (E) Fluorescent streak images of WBCs at various positions in the magnetic sorter, from inlet to outlet (insets 1–7). Inset 8 shows a fluorescent streak image of isolated CTCs at the product port. An image of the microfabricated magnetic sorter device is also shown. Reproduced from ref. 117 with permission from the authors. Originally published in PNAS, Copyright 2020 National Academy of Sciences.
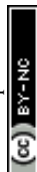
WBC extraction efficiency of 83.9%, and a cell viability of 96.6%, comparable to or exceeding conventional centrifugation methods. The IMF cube offers a robust, user-friendly alternative for WBC isolation, particularly in settings requiring compact and automated solutions.[69]

5.2. Immunoselection techniques

In a recent study, Hassan et al.[63] developed a point-of-care microfluidic biochip for quantifying CD64 expression from lysed whole blood, aimed at improving diagnosis and stratification of sepsis. Sepsis is a severe and often fatal condition that requires rapid and accurate diagnostic methods to ensure timely and appropriate treatment. CD64, a high-affinity Fcγ receptor expressed on neutrophils and monocytes, is upregulated in response to bacterial infection and systemic inflammation, making it a clinically relevant biomarker for early sepsis diagnosis. The biochip uses differential immunoaffinity capture to selectively isolated CD64+ cells, integrating a Coulter principle-based electrical counter and a microfluidic capture chamber. Whole blood is lysed using a buffer containing formic acid and saponin, followed by quenching to restore isotonic conditions. As shown in Fig. 4C, the system enables accurate enumeration and capture of CD64+ cells, with clinical validation demonstrating strong correlation with flow cytometry data. The platform supports real-time monitoring of leukocyte counts and CD64 expression, offering a rapid and reliable tool for bedside sepsis diagnostics.[63]

Nagrath et al.[116] developed a microfluidic chip for isolating and analyzing CTCs from lysed whole blood of cancer patients. The device captures viable epithelial tumor cells via antibody-coated microposts under controlled laminar flow. Microposts are functionalized with antibodies against epithelial cell adhesion molecule (EpCAM), enabling selective adhesion of carcinoma cells while excluding hematologic cells. The system employs a pneumatic pressure-regulated pump to drive continuously mixed blood through the chip, preventing cell sedimentation. As shown in Fig. 4D, the chip features silicon-etched microposts arranged in an equilateral triangular lattice with 50 μm spacing, optimized for capture efficiency. The platform enables direct CTC detection from peripheral blood collected via venipuncture, offering a minimally invasive alternative to tissue biopsy for longitudinal cancer monitoring.[116]

Performance evaluation demonstrated high sensitivity, with CTCs detected in 115 of 116 samples (99%), including all early-stage prostate cancer cases. The study processed blood volumes ranging from 0.9 to 5.1 mL, with the single negative result corresponded to the smallest volume (0.9 mL), suggesting a potential detection limit at low volumes. Fluorescence imaging of CTCs from NSCLC patients revealed malignant morphology—large size, high nuclear-to-cytoplasmic ratio, and visible nucleoli—distinguished from leukocytes using DAPI (a nuclear stain), cytokeratin (an epithelial cell marker), and CD45 (a leukocyte marker) staining. To assess preprocessing requirements, RBC lysis was performed using ammonium chloride, followed by

centrifugation and buffer resuspension. Capture rates from lysed and whole blood were comparable (Fig. 4D), indicating that the chip functions effectively without RBC pre-lysis. The device achieved ~50% purity and consistent CTC identification, underscoring its utility for streamlined, non-invasive cancer diagnostics and research.[116]

5.3. Hybrid techniques

Mishra et al.[117] developed the ^{LP}CTC-iChip, an ultrahigh-throughput microfluidic platform designed for isolating CTCs from leukapheresis products. This development is significant in the context of cancer diagnostics and treatment, as it allows for the efficient and rapid sorting of CTCs, which are crucial for monitoring cancer progression and response to treatment. The device employs a two-stage process, starting with filtration and inertial focusing to align cells, followed by magnetic deflection of WBCs labeled with magnetic beads. As illustrated in Fig. 4E, unlabeled CTCs are collected in a reduced volume after passing through a second set of sorting channels. The ^{LP}CTC-iChip rapidly sorts through an entire leukapheresis product of over 6 billion nucleated cells, increasing CTC isolation capacity by two orders of magnitude. The platform achieves >86% recovery of viable CTCs with $>10^5$-fold enrichment through sequential magnetic depletion of hematopoietic cells. It supports processing at 168 mL h^{-1}, enabling complete isolation of CTCs from a 65 mL leukapheresis product in under 3 hours. The device depletes >99.999% of RBCs and platelets and 99.97% of WBCs, yielding CTC purities of approximately 0.3%. These performance metrics are achieved while preserving the viability and proliferative capacity of isolated CTCs. The marker-independent design enables broad applicability across solid tumor types, supporting minimally-invasive cancer diagnostics and longitudinal monitoring.[117]

Advances in microfluidic technologies have enabled the effective use of lysed whole blood in these platforms, addressing limitations associated with traditional dilution-based methods. Passive, immunoselection, and hybrid techniques have demonstrated the utility of RBC lysis in enhancing imaging clarity, improving target cell accessibility, and streamlining workflows. However, many platforms such as those by Hassan et al.[63] and Mishra et al.[117] still rely on multi-step protocols, external pumping systems, or labeling strategies, which can hinder point-of-care deployment. Additionally, preprocessing steps like centrifugation and chemical quenching introduce variability and limit automation. To overcome these challenges, recent innovations such as the previously discussed PRECISE system by Ayers et al.[112] and the centrifugal microfluidic platform by Hatami et al.[113] have integrated on-chip lysis, target capture, and analysis into fully automated, electricity-free formats. The PRECISE platform combines plasma filtration, magnetic bead-based extraction, and digital PCR, delivering performance comparable to standard laboratory methods. It processes 50 μL of whole blood in just 16 minutes. In a proof-of-concept study using HCV-spiked blood, it achieved a detection limit of ~6770 IU mL^{-1}, meeting point-of-care

diagnostic standards. Similarly, Hatami's lab-on-a-disk device automates extraction of cell-free DNA directly from 3 mL of whole blood in 20 min, achieving 99% purity and accurate fetal sex identification using real-time PCR. These systems demonstrate the potential to streamline lysed whole blood processing, making it faster and more efficient. However, broader adoption in clinical diagnostics and monitoring will require overcoming challenges such as variability in sample quality, lack of standardization, and integration into existing clinical workflows.

6. Whole blood microfluidics

The separation of cellular components from whole blood a cornerstone of clinical diagnostics. While conventional approaches often rely on lysed or diluted blood to reduce viscosity and enhance cell visibility, they can introduce workflow complexity and variability. Recent advances in microfluidic technologies have enabled direct processing of whole blood without the need for lysis or dilution, simplifying procedures and preserving cellular integrity. Techniques such as inertial focusing, shear-induced

diffusion, and dielectrophoresis have significantly improved separation efficiency and purity. These innovations support the development of rapid, point-of-care diagnostic platforms by minimizing sample processing and maintaining high analytical fidelity.[118,119]

6.1. Passive techniques

The separation of cellular components from whole blood is a critical task in clinical diagnostics and point-of-care testing. Advanced microfluidic techniques have been developed to address the challenges associated with efficient separation of these components. Table 4 provides a summary of these methods. Kim *et al.*[120] developed a membrane filtration-based microfluidic device for plasma extraction from whole blood without external instrumentation. The system integrates a commercial membrane filter with a dual-cover microfluidic design to minimize leakage of residual blood cells. Nano-interstices (NIs) embedded on both sides of the channel enhance passive plasma extraction.[120] As shown in Fig. 5A, the device achieved a plasma yield of approximately 45% from 100 μL of whole blood within 16 min.[120] While

**Table 4** Comparison of microfluidic devices for cellular separation from whole blood

Device	Primary mechanism	Sample	Output	Key performance metrics	Limitations
Multi-flow microfluidic system[68]	Inertial migration	Lysed and diluted blood	CTCs	High purity (>87%) and efficiency (>99%) for CTC separation; recovery rate >93% at 50 cells per 5 mL blood	- Requires RBC lysis - Size overlap (CTC/WBC)
Membrane filtration-based microfluidic device[120]	Membrane filtration	Whole blood	Plasma	High extraction yield (~45%) within 16 minutes for 100 μL	- Time-consuming - Risk of membrane clogging
Shear-induced diffusion (SID) device[42]	Shear-induced diffusion	Whole blood	Leukocytes	High throughput and efficiency, size-dependent enrichment of WBCs	- Limited control over precise cell types - Overlap in size with large RBCs or small CTCs
CTC-iChip[125]	DLD + inertial focusing + magnetophoresis	Whole blood premixed with immunomagnetic beads	CTCs	High purity and yield of CTCs, high sensitivity and specificity	- Requires immunolabeling - Complex multi-step setup - Limited to known CTC markers
Elasto-inertial device[121]	Elasto-inertial focusing	Whole blood	Bacteria	76% recovery of bacteria, high separation efficiency	- Optimized for small targets (*e.g.*, bacteria) - Limited for larger/deformable cells
Inflection point focusing device[122]	Shear gradient lift force	Whole blood	CTCs	Efficient focusing of target cells without dilution or cell lysis	- Reduced efficiency at low flow rates - Size overlap with WBCs
Microfluidic chip for CTC capture and analysis[123]	Size-based capture with magnetic beads	Whole blood	CTCs and protein quantification	High capture efficiency (>95%), protein quantification	- Requires marker expression - Multi-step setup - Size overlap
Continuum sorting platform for tumor cells[124]	Magnetic sorting based on surface antibody expression	Whole blood	Tumor cell sub-populations	Effective isolation and analysis of tumor heterogeneity	- Marker-dependent - May miss antigen-negative subpopulations - Limited to known phenotypes

effective, the system is limited by relatively long processing times and potential membrane clogging during extended operation.

Zhou et al.[42] introduced a shear-induced diffusion (SID) approach for size-dependent enrichment of leukocytes from undiluted whole blood. High-speed imaging revealed that larger particles, such as WBCs, preferentially migrate laterally toward flow interfaces due to SID effects. Fig. 5B illustrates the migration trajectories of 18.7 μm particles in while blood,

highlighting distinct lateral migration patterns. Zhou et al.[42] demonstrated that the size-dependent lateral migration in whole blood is primarily results from differences in downstream particle velocity, which inversely scales with particle size. Using this principle, their platform achieved 2.6× enrichment of WBCs from whole blood with minimal preprocessing, increasing the WBC fraction from 0.17% to 0.44%. Notably, granulocytes were selectively enriched up to 87.2% while depleting lymphocytes to 4.01%. These results
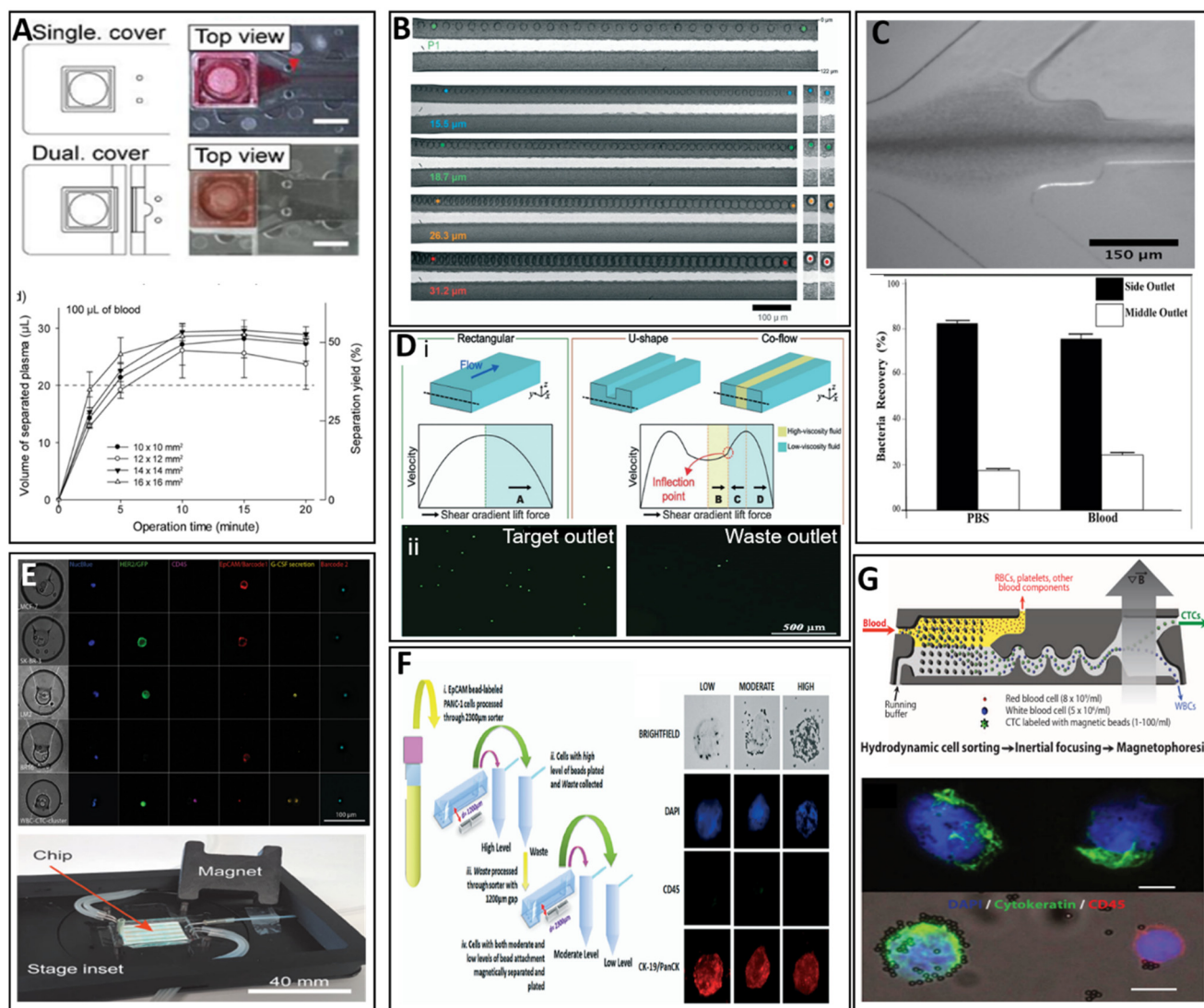
Fig. 5 Use of whole blood in microfluidics. (A) Whole blood application to single- and dual-cover devices. The red arrowhead indicates blood leakage. Scale bar, 4 mm. Reproduced from ref. 120 under a CC BY 4.0, Copyright 2021. (B) Demonstration of size-dependent migration of particles in whole blood using high-speed imaging for four particle sizes: 15.5 μm, 18.7 μm, 26.3 μm, and 31.2 μm diameter. Reproduced from ref. 42 with permission from the Royal Society of Chemistry. (C) Elasto-inertial focusing of blood cells in non-Newtonian fluid (PEO). Reproduced from ref. 121 under a CC BY 4.0, Copyright 2017. (D) (i) Velocity profile illustrations of different channel designs. (ii) Fluorescence microscopy images of the outlet region showing the spatial separation of fluorescently labeled HeLa cells. Reproduced from ref. 122 with permission from the Royal Society of Chemistry. (E) The microfluidic chip design and operation for CTC capture and analysis. Reproduced from ref. 123 under a CC BY 4.0, Copyright 2020. (F) Schematic of process used for isolating cells according to 3 varying levels of EpCAM. Brightfield and immunofluorescent images of CTCs isolated based on EpCAM expression levels. Scale bars represent 20 μm. Reproduced from ref. 124 with permission from the Royal Society of Chemistry. (G) CTC-iChip system can be operated in positive isolation (shown) or negative depletion mode. The images demonstrate the detailed cellular analysis and imaging capabilities of the posCTC-iChip. Reproduced from ref. 125 Copyright 2013 American Association for the Advancement of Science.

highlight the platform's potential for high-throughput, size-based cell separation directly from whole blood, offering a simplified workflow for applications such as CTC isolation. However, overlapping size distributions between target and non-target cells and complex flow behaviors may affect separation consistency.

Faridi et al.[121] demonstrated an elasto-inertial microfluidic approach for label-free bacterial separation from whole blood, targeting sepsis diagnostics. This technique leverages viscoelastic and inertial forces to focus blood cells at the channel centerline while directing bacteria to side outlets. Fig. 5C illustrates the migration of blood cells in a non-Newtonian fluid, where blood cells are focused at the centerline of the channel, with 76% of bacteria recovered at the side outlet. Faridi et al.[121] demonstrated the potential of elasto-inertial microfluidics for clinical diagnostics, particularly in the rapid and label-free separation of bacteria from whole blood. Before testing with biological samples, the system was optimized using microparticles, achieving recovery rates of 95% for 5 μm particles and 93% for 2 μm particles, validating its size-based separation capability. This technique ensures high separation efficiency and purity, providing a valuable tool for diagnosing sepsis and potentially other bloodstream infections. Nevertheless, limitations include reduced performance for larger or deformable targets and sensitivity to flow rate and fluid properties.

Lee et al.[122] developed an inertial microfluidic technique termed inflection point focusing for separation of rare cells from untreated whole blood. This method uses shear gradient lift force, modulated by channel geometry and co-flowing fluids with different viscosities, to focus target cells at velocity profile inflection points. Fig. 5D illustrates the 3D channel geometry and velocity profiles for rectangular, U-shaped, and co-flow channels, highlighting how the shear gradient lift force is redirected at inflection points. Fluorescence microscopy image of labeled HeLa cells at the outlet region demonstrates enrichment with 92.6% efficiency at 50 μL min⁻¹. These attributes make the platform particularly suitable for clinical applications such as liquid biopsy and rare cell diagnostics, where rapid, label-free, and high-purity enrichment of CTCs directly from whole blood is essential.[122] Despite its efficiency, the inflection point focusing device may experience reduced performance at low flow rates and could face challenges when separating CTCs with overlapping size compared to WBCs.

6.2. Immunoselection techniques

Armbrecht et al.[123] developed a microfluidic platform for the integrated capture, isolation, and protein analysis of CTCs. The chip design, shown in Fig. 5E, includes a magnetic lid and analysis chambers for co-capture of CTCs and functionalized magnetic beads. Using spiked cancer cell lines introduced directly into the chip, the system achieved >95% capture efficiency and enabled quantification of secreted

proteins such as granulocyte colony-stimulating factor (G-CSF), with a detection limit below 3700 molecules per cell. G-CSF can promote neutrophil recruitment and immune modulation, contributing to tumor progression and metastasis. Monitoring such secretions can offer functional biomarkers for prognosis and therapeutic decision-making. Brightfield and fluorescence images also reveal the presence of nucleated cells and the expression of membrane proteins HER-2, EpCAM, and CD45. This platform supports functional profiling of CTCs, offering insights into tumor progression and therapeutic response. However, reliance on size-based capture and immunomagnetic labeling may exclude smaller or less rigid CTC subtypes.

Jack et al.[124] developed a microfluidic system for the continuum sorting of tumor cell sub-populations based on surface antibody expression levels. The platform uses magnetic field gradients to separate cells with varying bead coverage, reflecting differential EpCAM expression. Fig. 5F presents a schematic of the process used for isolating cells according to three varying levels of EpCAM expression, demonstrating how the cells' invasive potential is assessed based on their EpCAM levels. Immunofluorescent images of CTCs sorted into low, moderate, and high EpCAM expression groups are also shown. This method enables detailed analysis of tumor heterogeneity and invasive potential. However, reliance on specific surface marker expression suggests that CTCs lacking the targeted surface markers may be missed.

6.3. Hybrid techniques

Ozkumur et al.[125] developed the CTC-iChip, a multi-stage microfluidic platform combining DLD, inertial focusing, and magnetophoresis for CTC isolation. As shown in Fig. 5G, the system processes whole blood pre-mixed with immunomagnetic beads, sequentially removing RBCs and platelets, aligning nucleated cells, and magnetically separating labeled CTCs. The chip can process 8 mL of whole blood in 1 hour, achieving CTC recovery rates of 97%. In positive selection mode, magnetically labeled CTCs are retained while unlabeled blood cells are removed, resulting in >3.5 log leukocyte depletion (mean of 1500 WBCs per mL). In contrast, negative selection mode depletes labeled leukocytes and enriches unlabeled CTCs, achieving 2.5-log depletion (mean of 32 000 WBCs per mL). This approach enables high-throughput, high-purity CTC isolation suitable for downstream molecular analyses. Despite its strengths, the CTC-iChip requires pre-labeling of target cells with immunomagnetic beads and involves a complex multi-step setup, which may limit its clinical scalability.

While these microfluidic systems represent significant progress in processing of whole blood, several limitations persist. Membrane-based devices may suffer from clogging and limited flow rates. Similarly, SID and DEP-based methods require precise tuning and may lack robustness under variable conditions. To address these challenges, recent innovations have introduced vortex-enhanced spiral microchannels[126] and gravity-assisted platforms[127] that enable clog-free plasma

separation and passive isolation of platelet-rich plasma without the need for external pumps. These systems leverage microchannel geometry and flow-driven design to simplify operation, reduce mechanical complexity, and support low-cost, point-of-care diagnostic applications.

7. Challenges and future perspectives

7.1. Current challenges

Handling whole blood in microfluidic applications presents a range of unique challenges that must be addressed to enhance the accuracy, reliability, and scalability of diagnostic tools. Among the primary issues is the propensity for blood to form microclots, even in EDTA-coated collection tubes, which can lead to clogging of microfluidic channels. The intricate cellular composition of blood also increases the risk of lysis due to fluidic shear, further leading to clogging in microfluidic channels. This not only disrupts device functionality but also limits throughput, especially when processing larger sample volumes (i.e., more than 1–2 standard blood draw tubes). Gifford et al.[128] demonstrated a system utilizing blood bags integrated with continuous filtration, effectively preventing clogging and ensuring sterility when working with large blood volumes. Strategies like dilution or off-chip cell lysis can mitigate clogging as well, but add complexity to the workflow.

Activation of blood components, particularly platelets and white blood cells, presents a significant challenge in microfluidic systems. This activation can be triggered by factors such as shear stress, prolonged residence time, or interactions with microchannel surfaces. To mitigate these effects, several strategies are used, including the use of chemical stabilizers such as EDTA, optimizing channel designs to minimize cell–surface interactions, and reducing the time cells spend within the device.[115] As a result, continuous-flow systems such as acoustophoresis and inertial microfluidics are generally favored for blood handling due to their low-shear, high-throughput characteristics. In contrast, systems with complex microstructures, such as filtration arrays, pose a higher risk of clogging and cellular activation due to their confined geometries and slower flow rates. Similarly, immunoselection platforms, which often rely on creeping flow to enhance binding efficiency, may increase activation risk due to extended cell residence times. Future designs of microfluidic systems must prioritize hemocompatible architectures that balance high throughput with minimal mechanical and chemical disturbance to blood components.

Sterility is another critical consideration, particularly in clinical applications. Open systems, such as syringe pumps, pose a risk of contamination, making them unsuitable for clinical use. Closed systems, such as blood bags integrated with continuous filtration mechanisms, offer a promising alternative. Recent advances, as described by Gifford et al.[128] in their work on leukocyte enrichment using blood bags, demonstrate the potential of these approaches to improve

both sterility and sample integrity. Blood cells may also deform under shear stress in microchannels, and while this characteristic can be advantageous for specific applications like cell sorting, it can also lead to cell activation and mechanical damage. Designing microfluidic environments that replicate physiological flow conditions may mitigate these challenges and improve the robustness of analyses. Recent advancements in microchannel geometry and flow stabilization methods, as noted by Jiang et al.,[129] have shown promise in reducing shear-induced deformation.

The non-Newtonian nature of blood adds another layer of complexity. Its variable flow properties can make it challenging to maintain consistent flow rates, especially in the narrow channels typical of microfluidic devices. This variability can impact assay precision and compromise the reproducibility of results. Addressing this issue may involve advanced computational modeling and the development of shear-thinning additives. Lu et al.[38] have highlighted the use of shear-rate-dependent designs that optimize flow dynamics, potentially providing more consistent performance in microfluidic devices.[38] Coating channels with biocompatible materials or employing inert carrier fluids could also be effective at limiting the impacts of non-specific interactions of blood proteins and bioactive molecules with microfluidic channel surfaces. Gonçalves et al.[130] emphasized the significance of surface modification techniques in enhancing the hydrophilicity of PDMS microfluidic devices and concluded that bulk modification with 2.5% polyethylene oxide (PEO) was the most effective. This method improved wettability, reduced the water contact angle, and maintained optical transparency, making it superior to other surfactants such as polyethylene glycol (PEG) and Pluronic F127.

Finally, the stability of blood samples is a broader challenge that extends beyond microfluidics. Delays between blood collection and analysis can lead to cell death, debris formation, and increased clogging. Rossi et al.[29] highlighted the use of stabilization agents, such as bovine serum albumin (BSA), which was used to passivate the polymer surface of the microfluidic chip. This prevents undesired contact pathway activation in treated blood and mitigates air bubbles during perfusion, maintaining sample integrity over time in point-of-care systems to maintain sample viability over extended periods. Components like CTCs and cDNA are highly susceptible to degradation, and specialized collection tubes must be used to preserve these components during transport.

7.2. Future directions

Given the aforementioned challenges, a key future direction for whole blood microfluidics lies in automation and integration. The development of microfluidic devices capable of handling whole blood with minimal sample preparation is essential. An illustrative example is the CTC-iChip,[125] which demonstrates the potential of leveraging diverse microfluidic technologies to create more efficient and automated systems.

Devices capable of operating directly with whole blood, without needing dilution or lysis, could significantly simplify workflows, which is especially valuable in point-of-care settings. Reducing the delays between sample collection and testing is increasingly important, as fresh samples reduce cell death, debris formation, and clotting, thereby ensuring better performance and test accuracy. Future devices could integrate parallelization to mitigate these challenges and further expedite sample processing.

The increased use of microfluidic devices in clinical practice will necessitate seamless integration with existing workflows. Future developments should aim to produce devices that complement or replace current procedures without disrupting established practices. Enhancing the accuracy and reliability of microfluidic devices involves accounting for variations in blood samples due to patient conditions, time points, and collection methods. Standardizing procedures and integrating artificial intelligence (AI) for pattern recognition could mitigate these issues. The development of low-cost, minimally invasive, and portable devices for point-of-care blood diagnostics can enhance healthcare accessibility, particularly in underserved and resource-limited communities. Such devices have the potential to replace conventional clinical instruments, bringing diagnostics closer to patients.

Technological advances are poised to transform microfluidic devices for whole blood analysis. Innovations in biocompatible coatings and closed systems, such as blood bags, can reduce clogging and enhance sterility.[128] High-throughput designs, AI-driven flow control, and stabilization of components like CTCs and cDNA will ensure reliability during transport and analysis.[29] Portable, automated devices and their integration with imaging techniques hold promise for improved point-of-care diagnostics. Cost-effective manufacturing methods, such as 3D printing, will further drive scalability, making these technologies widely accessible and impactful for healthcare.

7.3. Opportunities for AI

In recent years, rapid advancements in artificial intelligence (AI) and machine learning (ML) have led to their widespread adoption across numerous fields, including drug development and disease diagnostics. In microfluidics, AI/ML hold significant promise for reducing the cost and time associated with device design, experimentation, and optimization – ultimately driving toward greater automation. This includes the development of ML models capable of predicting blood cell dynamics for applications such as sorting, separation, and focusing. These intelligent systems can analyze key cellular properties, including shape and mechanical stiffness, offering researchers a deeper understanding of cell behavior in various medical contexts.[131]

By enabling such automation, AI/ML can greatly accelerate the development and deployment of next-generation microfluidic devices. A notable example of this integration is the use of ML to optimize microchannel geometries through CFD-informed algorithms. For example, Manekar *et al.*[132]

applied ML techniques to refine passive microfluidic designs under varying flow conditions. The optimized configurations achieved yields of 90–95%, demonstrating the power of AI to enhance fluid handling and support effective device engineering.

In the context of cellular analysis, AI-enabled microfluidic cytometers have emerged as powerful tools for rapid and accurate quantification of cell types. For instance, a recent study[133] introduced a microfluidic cytometer capable of quantifying CD4+ T cells in human blood samples with high accuracy, comparable to traditional flow cytometry, while requiring less analysis time and smaller sample volumes. Additionally, AI has been applied to analyze RBC dynamics within microfluidic channels. Rizzuto *et al.*[134] combined microfluidics with ML to develop a device that mimics the spleen's filtering function, enabling the classification of RBCs in rare hereditary hemolytic anemia with 91% efficiency. This approach facilitates more precise diagnostics and informs treatment strategies.

These examples highlight the transformative potential of AI/ML in enhancing the capabilities of microfluidic devices for blood analysis. By enabling automated design optimization, real-time monitoring, and precise cellular characterization, AI-integrated microfluidics is poised to revolutionize diagnostics and personalized healthcare. Furthermore, the integration of AI with high-throughput microfluidic platforms opens new opportunities for large-scale, data-driven discovery in hematology and disease profiling.

8. Concluding remarks

Microfluidic technologies have transformed biomedical analysis, offering unprecedented precision, integration, and miniaturization for blood-based diagnostics. These systems have emerged as versatile platforms for blood sample handling, cell separation, and biomarker detection on the microscale. In this review, we examined how different blood preparation methods – including diluted, whole, lysed, and lysed-diluted samples – interact with microfluidic designs and influence device performance.

We reviewed a wide range of cell separation techniques, including inertial microfluidics, deterministic lateral displacement, magnetic separation, membrane-based filtration, hydrodynamic focusing, viscoelastic flow sorting, and capillary-driven separation. Each method offers distinct operational advantages depending on the clinical application and target analytes, underscoring the adaptability of microfluidic platforms to diverse diagnostic needs.

As these technologies move closer to clinical translation, performance must be evaluated not only by separation efficiency but also by operational robustness in complex biological fluids such as whole blood. While many systems perform reliably under controlled conditions, real-world samples introduce additional challenges, such as clogging, hemolysis, and unintended cell activation, which can compromise analytical fidelity. These effects are closely tied to

flow rate, surface interactions, and residence time, and must be considered during device design, particularly for high-throughput or continuous-flow applications. Furthermore, biological variability, including differences in hematocrit, plasma viscosity, and cellular composition, can significantly influence microfluidic behavior in ways that are not always predictable.

Future progress will require a holistic design approach that integrates both mechanical precision and hemocompatibility to ensure consistent and safe performance under clinically relevant conditions.[135] Looking ahead, the field is moving toward fully integrated, automated, and intelligent microfluidic systems. Positioned at the intersection of engineering and medicine, microfluidics is now a cornerstone of biomedical innovation, bridging the gap between laboratory research and real-world clinical implementation. These advances hold promise for enabling more personalized and timely diagnostics, although their broader adoption in clinical and research settings will depend on continued validation and seamless integration into routine practice.

Conflicts of interest

There are no conflicts to declare.

Data availability

All relevant data are described within the manuscript.

Acknowledgements

References

1 J. Mukherjee, D. Chaturvedi, S. Mishra, R. Jain and P. Dandekar, Microfluidic technology for cell biology–related applications: a review, *J. Biol. Phys.*, 2024, **50**(1), 1–27.

2 N. Xiang and Z. Ni, Microfluidics for Biomedical Applications, *Biosensors*, 2023, **13**(2), 161.

3 K. W. Oh, Microfluidic Devices for Biomedical Applications: Biomedical Microfluidic Devices 2019, *Micromachines*, 2020, **11**(4), 370.

4 D. K. Patel, M. M. Espinal, T. V. Patil, K. Ganguly, S. D. Dutta and R. Luthfikasari, *et al.*, Microfluidics and Lab-on-a-Chip for Biomedical Applications, in *Nanorobotics and Nanodiagnostics in Integrative Biology and Biomedicine*, ed. K. T. Lim and K. A. Abd-Elsalam, Springer International Publishing, Cham, 2023, pp. 263–283, DOI: 10.1007/978-3-031-16084-4_11.

5 D. D. Carlo, Inertial microfluidics, *Lab Chip*, 2009, **9**(21), 3038–3046.

6 A. A. S. Bhagat, S. S. Kuntaegowdanahalli and I. Papautsky, Continuous particle separation in spiral microchannels using dean flows and differential migration, *Lab Chip*, 2008, **8**(11), 1906–1914.

7 L. R. Huang, E. C. Cox, R. H. Austin and J. C. Sturm, Continuous particle separation through deterministic lateral displacement, *Science*, 2004, **304**(5673), 987–990.

8 N. Pamme, Magnetism and microfluidics, *Lab Chip*, 2006, **6**(1), 24–38.

9 Y. Fan, X. Wang, J. Ren, F. Lin and J. Wu, Recent advances in acoustofluidic separation technology in biology, *Microsyst. Nanoeng.*, 2022, **8**(1), 1–16.

10 Y. Gao, M. Wu, Y. Lin and J. Xu, Acoustic Microfluidic Separation Techniques and Bioapplications: A Review, *Micromachines*, 2020, **11**(10), 921.

11 P. Su, C. Ren, Y. Fu, J. Guo, J. Guo and Q. Yuan, Magnetophoresis in microfluidic lab: Recent advance, *Sens. Actuators, A*, 2021, **332**, 113180.

12 F. Alnaimat, S. Dagher, B. Mathew, A. Hilal-Alnqbi and S. Khashan, Microfluidics Based Magnetophoresis: A Review, *Chem. Rec.*, 2018, **18**(11), 1596–1612.

13 S. Y. Jung, J. E. Park, T. G. Kang and K. H. Ahn, Design Optimization for a Microfluidic Crossflow Filtration System Incorporating a Micromixer, *Micromachines*, 2019, **10**(12), 836.

14 K. D. Lenz, S. Jakhar, J. W. Chen, A. S. Anderson, D. C. Purcell and M. O. Ishak, *et al.*, A centrifugal microfluidic cross-flow filtration platform to separate serum from whole blood for the detection of amphiphilic biomarkers, *Sci. Rep.*, 2021, **11**(1), 5287.

15 M. Yamada and M. Seki, Hydrodynamic filtration for on-chip particle concentration and classification utilizing microfluidics, *Lab Chip*, 2005, **5**(11), 1233–1239.

16 H. Zhang, H. Chang and P. Neuzil, DEP-on-a-Chip: Dielectrophoresis Applied to Microfluidic Platforms, *Micromachines*, 2019, **10**(6), 423.

17 A. Boussommier-Calleja, R. Li, M. B. Chen, S. C. Wong and R. D. Kamm, Microfluidics: A new tool for modeling cancer-immune interactions, *Trends Cancer*, 2016, **2**(1), 6–19.

18 Y. F. S. Seah, H. Hu and C. A. Merten, Microfluidic single-cell technology in immunology and antibody screening, *Mol. Aspects Med.*, 2018, **59**, 47–61.

19 N. Xiang and Z. Ni, Inertial microfluidics: current status, challenges, and future opportunities, *Lab Chip*, 2022, **22**(24), 4792–4804.

20 D. Huang, J. Man, D. Jiang, J. Zhao and N. Xiang, Inertial microfluidics: Recent advances, *Electrophoresis*, 2020, **41**(24), 2166–2187.

21 A. Hochstetter, R. Vernekar, R. H. Austin, H. Becker, J. P. Beech and D. A. Fedosov, *et al.*, Deterministic Lateral Displacement: Challenges and Perspectives, *ACS Nano*, 2020, **14**(9), 10784–10795.

22 O. Civelekoglu, A. B. Frazier and A. F. Sarioglu, The Origins and the Current Applications of Microfluidics-Based Magnetic Cell Separation Technologies, *Magnetochemistry*, 2022, **8**(1), 10.

23 G. Lippi and M. Plebani, Laboratory abnormalities in patients with COVID-2019 infection, *Clin. Chem. Lab. Med.*, 2020, **58**(7), 1131–1134.

24 W. A. Al-Soud and P. Rådström, Purification and Characterization of PCR-Inhibitory Components in Blood Cells, *J. Clin. Microbiol.*, 2001, **39**, 485–493.

25 B. J. Bain, *Morphology of Blood Cells, in Blood Cells*, ed. B. J. Bain, John Wiley & Sons, 2014, ch. 3, pp. 67–185.

26 R. A. McPherson and M. R. Pincus, *Henry's Clinical Diagnosis and Management by Laboratory Methods*, Elsevier, St. Louis, 24th edn, 2021, ISBN: 9780323673204.

27 A. V. Hoffbrand and P. A. H. Moss, *Hoffbrand's essential haematology*, John Wiley & Sons, Chinester, West Sussex, 7th edn, 2016, p. 1, (Essentials (Wiley-Blackwell (Firm))), available from: http://www.credoreference.com/book/wileyhh.

28 J. P. Greer, D. A. Arber, B. E. Glader, A. F. List, R. T. Means and G. M. Rodgers, *et al.*, *Wintrobe's clinical hematology*, Wolters Kluwer Health Pharma Solutions (Europe) Ltd, 14th edn, 2018, available from: http://www.scopus.com/inward/record.url?scp=85063312829&partnerID=8YFLogxK.

29 S. L. Diamond and J. M. Rossi, Point of care whole blood microfluidics for detecting and managing thrombotic and bleeding risks, *Lab Chip*, 2021, **21**(19), 3667–3674.

30 A. Tavakolidakhrabadi, M. Stark, U. Bacher, M. Legros and C. Bessire, Optimization of Microfluidics for Point-of-Care Blood Sensing, *Biosensors*, 2024, **14**(6), 266.

31 X. Fang, C. Sun, P. Dai, Z. Xian, W. Su and C. Zheng, *et al.*, Capillary Force-Driven Quantitative Plasma Separation Method for Application of Whole Blood Detection Microfluidic Chip, *Micromachines*, 2024, **15**(5), 619.

32 W. C. Lee, H. Y. Ng, C. Y. Hou, C. T. Lee and L. M. Fu, Recent advances in lab-on-paper diagnostic devices using blood samples, *Lab Chip*, 2021, **21**(8), 1433–1453.

33 M. Toner and D. Irimia, Blood-on-a-chip, *Annu. Rev. Biomed. Eng.*, 2005, **7**, 77–103.

34 F. Cui, M. Rhee, A. Singh and A. Tripathi, Microfluidic Sample Preparation for Medical Diagnostics, *Annu. Rev. Biomed. Eng.*, 2015, **17**(1), 267–286.

35 K. Torres-Castro, K. Acuña-Umaña, L. Lesser-Rojas and D. R. Reyes, Microfluidic Blood Separation: Key Technologies and Critical Figures of Merit, *Micromachines*, 2023, **14**(11), 2117.

36 H. Kim, A. Zhbanov and S. Yang, Microfluidic Systems for Blood and Blood Cell Characterization, *Biosensors*, 2023, **13**(1), 13.

37 L. M. Rey Gomez, R. Hirani, A. Care, D. W. Inglis and Y. Wang, Emerging Microfluidic Devices for Sample Preparation of Undiluted Whole Blood to Enable the Detection of Biomarkers, *ACS Sens.*, 2023, **8**(4), 1404–1421.

38 N. Lu, H. M. Tay, C. Petchakup, L. He, L. Gong and K. K. Maw, *et al.*, Label-free microfluidic cell sorting and detection for rapid blood analysis, *Lab Chip*, 2023, **23**(5), 1226–1257.

39 P. Yu, S. Zhu, Y. Luo, G. Li, Y. Pu and B. Cai, *et al.*, Application of Circulating Tumor Cells and Circulating Free DNA from Peripheral Blood in the Prognosis of Advanced Gastric Cancer, *J. Oncol.*, 2022, **2022**, 9635218.

40 J. D'Silva, R. H. Austin and J. C. Sturm, Inhibition of clot formation in deterministic lateral displacement arrays for processing large volumes of blood for rare cell capture, *Lab Chip*, 2015, **15**(10), 2240–2247.

41 N. Xiang, J. Wang, Q. Li, Y. Han, D. Huang and Z. Ni, Precise Size-Based Cell Separation via the Coupling of Inertial Microfluidics and Deterministic Lateral Displacement, *Anal. Chem.*, 2019, **91**(15), 10328–10334.

42 J. Zhou and I. Papautsky, Size-dependent enrichment of leukocytes from undiluted whole blood using shear-induced diffusion, *Lab Chip*, 2019, **19**(20), 3416–3426.

43 J. Zhou, C. Tu, Y. Liang, B. Huang, Y. Fang and X. Liang, *et al.*, Isolation of cells from whole blood using shear-induced diffusion, *Sci. Rep.*, 2018, **8**(1), 9411.

44 Y. Chen, M. Wu, L. Ren, J. Liu, P. H. Whitley and L. Wang, *et al.*, High-throughput acoustic separation of platelets from whole blood, *Lab Chip*, 2016, **16**(18), 3466–3472.

45 A. Urbansky, P. Ohlsson, A. Lenshof, F. Garofalo, S. Scheding and T. Laurell, Rapid and effective enrichment of mononuclear cells from blood using acoustophoresis, *Sci. Rep.*, 2017, **7**(1), 17161.

46 E. Undvall Anand, C. Magnusson, A. Lenshof, Y. Ceder, H. Lilja and T. Laurell, Two-Step Acoustophoresis Separation of Live Tumor Cells from Whole Blood, *Anal. Chem.*, 2021, **93**(51), 17076–17085.

47 Y. Wang, B. B. Nunna, N. Talukder and E. S. Lee, Microfluidic-Based Novel Optical Quantification of Red Blood Cell Concentration in Blood Flow, *Bioengineering*, 2022, **9**(6), 247.

48 W. Brakewood, K. Lee, L. Schneider, R. Lawandy and A. Tripathi, A capillary flow-driven microfluidic device for point-of-care blood plasma separation, *Front. Lab Chip Technol.*, 2022, **1**, 1051552.

49 M. Ranucci, T. Laddomada, M. Ranucci and E. Baryshnikova, Blood viscosity during coagulation at different shear rates, *Physiol. Rep.*, 2014, **2**(7), e12065.

50 E. Nader, S. Skinner, M. Romana, R. Fort, N. Lemonne and N. Guillot, *et al.*, Blood Rheology: Key Parameters, Impact on Blood Flow, Role in Sickle Cell Disease and Effects of Exercise, *Front. Physiol.*, 2019, **10**, 1329.

51 H. N. Iskandar and M. A. Ciorba, Biomarkers in inflammatory bowel disease: current practices and recent advances, *Transl. Res.*, 2012, **159**(4), 313–325.

52 M. Cristofanilli, G. T. Budd, M. J. Ellis, A. Stopeck, J Matera and M. C. Miller, *et al.*, Circulating tumor cells, disease progression, and survival in metastatic breast cancer, *N. Engl. J. Med.*, 2004, **351**(8), 781–791.

53 C. Alix-Panabières and K. Pantel, Challenges in circulating tumour cell research, *Nat. Rev. Cancer*, 2014, **14**(9), 623–631.

54 J. Lee, O. Sul and S. B. Lee, Enrichment of Circulating Tumor Cells from Whole Blood Using a Microfluidic Device for Sequential Physical and Magnetophoretic Separations, *Micromachines*, 2020, **11**(5), 481.

55 Y. Song, T. Tian, Y. Shi, W. Liu, Y. Zou and T. Khajvand, *et al.*, Enrichment and single-cell analysis of circulating tumor cells, *Chem. Sci.*, 2017, **8**(3), 1736–1751.

56 P. Bankó, S. Y. Lee, V. Nagygyörgy, M. Zrínyi, C. H. Chae and D. H. Cho, *et al.*, Technologies for circulating tumor cell separation from whole blood, *J. Hematol. Oncol.*, 2019, **12**(1), 48.
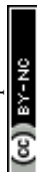
57 K. E. O'Connell, A. M. Mikkola, A. M. Stepanek, A. Vernet, C. D. Hall and C. C. Sun, *et al.*, Practical murine hematopathology: a comparative review and implications for research, *Comp. Med.*, 2015, **65**(2), 96–113.

58 Differential Blood Count: Reference Range, Interpretation, Collection and Panels, 2023 Oct 24 [cited 2025 Apr 17], available from: **https://emedicine.medscape.com/article/2085133-overview**.

59 A. Tigner, S. A. Ibrahim and I. V. Murray, *Histology, White Blood Cell*, StatPearls Publishing, Treasure Island, FL, 2024, available from: **http://www.ncbi.nlm.nih.gov/books/NBK563148/**.

60 M. Diez-Silva, M. Dao, J. Han, C. T. Lim and S. Suresh, Shape and Biomechanical Characteristics of Human Red Blood Cells in Health and Disease, *MRS Bull.*, 2010, **35**(5), 382–388.

61 T. Fukuda, E. Asou, K. Nogi and K. Goto, Evaluation of mouse red blood cell and platelet counting with an automated hematology analyzer, *J. Vet. Med. Sci.*, 2017, **79**(10), 1707–1711.

62 M. Ehtashamul Haque, A. J. Conde, W. N. MacPherson, S. R. Knight, R. M. Carter and M. Kersaudy-Kerhoas, A microfluidic finger-actuated blood lysate preparation device enabled by rapid acoustofluidic mixing, *Lab Chip*, 2023, **23**(1), 62–71.

63 U. Hassan, T. Ghonge, B. Reddy, M. Patel, M. Rappleye and I. Taneja, *et al.*, A point-of-care microfluidic biochip for quantification of CD64 expression from whole blood for sepsis stratification, *Nat. Commun.*, 2017, **8**(1), 15949.

64 M. Shehadul Islam, A. Aryasomayajula and P. R. Selvaganapathy, A Review on Macroscale and Microscale Cell Lysis Methods, *Micromachines*, 2017, **8**(3), 83.

65 S. H. Au, J. Edd, A. E. Stoddard, K. H. K. Wong, F. Fachin and S. Maheswaran, *et al.*, Microfluidic Isolation of Circulating Tumor Cell Clusters by Size and Asymmetry, *Sci. Rep.*, 2017, **7**(1), 2433.

66 E. J. Lim, T. J. Ober, J. F. Edd, G. H. McKinley and M. Toner, Visualization of microscale particle focusing in diluted and whole blood using particle trajectory analysis, *Lab Chip*, 2012, **12**(12), 2199.

67 Red Blood Cell Lysis Solution (10×)|Miltenyi Biotec|USA, [cited 2025 Jan 11], available from: **https://www.miltenyibiotec.com/US-en/products/red-blood-cell-lysis-solution-10x-1628.html**.

68 J. Zhou, A. Kulasinghe, A. Bogseth, K. O'Byrne, C. Punyadeera and I. Papautsky, Isolation of circulating tumor cells in non-small-cell-lung-cancer patients using a multi-flow microfluidic channel, *Microsyst. Nanoeng.*, 2019, **5**(1), 8.

69 S. Zhu, D. Wu, Y. Han, C. Wang, N. Xiang and Z. Ni, Inertial microfluidic cube for automatic and fast extraction of white blood cells from whole blood, *Lab Chip*, 2020, **20**(2), 244–252.

70 ACK Lysing Buffer, [cited 2025 Jan 11], available from: **https://www.thermofisher.com/order/catalog/product/A1049201**.

71 Z. Zhu, D. Wu, S. Li, Y. Han, N. Xiang and C. Wang, *et al.*, A polymer-film inertial microfluidic sorter fabricated by jigsaw puzzle method for precise size-based cell separation, *Anal. Chim. Acta*, 2021, **1143**, 306–314.

72 Biologos -, 2024 [cited 2025 Jan 11], ACK Lysis Buffer – Biologos, available from: **https://biologos.com/product/ack-lysis-buffer/**.

73 D. Di Carlo, K. H. Jeong and L. P. Lee, Reagentless mechanical cell lysis by nanoscale barbs in microchannels for sample preparation, *Lab Chip*, 2003, **3**(4), 287–291.

74 L. R. Blauch, Y. Gai, J. W. Khor, P. Sood, W. F. Marshall and S. K. Y. Tang, Microfluidic guillotine for single-cell wound repair studies, *Proc. Natl. Acad. Sci. U.S.A.*, 2017, **114**(28), 7283–7288.

75 H. Ramachandraiah, H. A. Svahn and A. Russom, Inertial microfluidics combined with selective cell lysis for high throughput separation of nucleated cells from whole blood, *RSC Adv.*, 2017, **7**(47), 29505–29514.

76 Y. J. Lo and U. Lei, A Continuous Flow-through Microfluidic Device for Electrical Lysis of Cells, *Micromachines*, 2019, **10**(4), 247.

77 C. P. Jen, J. H. Hsiao and N. A. Maslov, Single-Cell Chemical Lysis on Microfluidic Chips with Arrays of Microwells, *Sensors*, 2012, **12**(1), 347–358.

78 BestProtocols: Red Blood Cell Lysis Protocols Using eBioscience Lysis Buffers - US, [cited 2025 Jan 11], available from: **https://www.thermofisher.com/us/en/home/references/protocols/cell-and-tissue-analysis/protocols/red-blood-cell-lysis.html**.

79 PRIME PubMed | Micropillar array chip for integrated white blood cell isolation and PCR, [cited 2025 Jan 11], available from: **https://www.unboundmedicine.com/medline/citation/15748689/Micropillar_array_chip_for_integrated_white_blood_cell_isolation_and_PCR_**.

80 H. M. Ji, V. Samper, Y. Chen, C. K. Heng, T. M. Lim and L. Yobas, Silicon-based microfilters for whole blood cell separation, *Biomed. Microdevices*, 2008, **10**(2), 251–257.

81 E. Grigorov, B. Kirov, M. B. Marinov and V. Galabov, Review of Microfluidic Methods for Cellular Lysis, *Micromachines*, 2021, **12**, 498, available from: **https://www.ncbi.nlm.nih.gov/pmc/articles/PMC8145176/**.

82 S. Mehraji and D. L. DeVoe, Microfluidic synthesis of lipid-based nanoparticles for drug delivery: recent advances and opportunities, *Lab Chip*, 2024, **24**(5), 1154–1174.

83 H. W. Hou, A. A. S. Bhagat, W. C. Lee, S. Huang, J. Han and C. T. Lim, Microfluidic Devices for Blood Fractionation, *Micromachines*, 2011, **2**(3), 319–343.

84 K. Grindulis, N. G. Matusevica, V. Kozlova, R. Rimsa, K. Klavins and G. Mozolevskis, Sorption and release of small molecules in PDMS and COC for Organs on chip, *Sci. Rep.*, 2025, **15**(1), 14012.

85 A. R. Hyler, D. E. Thomas, K. S. Kinskie, K. M. Brown, J. L. Duncan and J. Cemazar, *et al.*, Characterizing Recent PDMS Changes in Electrokinetic-Based Microfluidic Devices' Performance and Manufacturing for Cell Sorting Applications, *Electrophoresis*, 2025, **44**, e8113.

86 V. Guarino, E. Perrone, A. Zizzari, M. Bianco, G. Giancane and R. Rella, *et al.*, Controlling endotoxin contamination in PDMS-based microfluidic systems for organ-on-chip technologies, *Polym. Test.*, 2025, **147**, 108795.

87 K. Ren, J. Zhou and H. Wu, Materials for Microfluidic Chip Fabrication, *Acc. Chem. Res.*, 2013, **46**(11), 2396–2406.

88 ISO - 11.080.01 - Sterilization and disinfection in general, [cited 2024 May 15], available from: https://www.iso.org/ics/11.080.01/x/.

89 S. C. Skaalure, S. C. Oppegard and D. T. Eddington, Characterization of sterilization techniques on a microfluidic oxygen delivery device, *Journal of Undergraduate Research at the University of Illinois at Chicago*, 2008, **2**(1), DOI: 10.5210/jur.v2i1.7462.

90 H. Mansour, E. A. Soliman, A. M. F. El-Bab, Y. Matsushita and A. L. Abdel-Mawgood, Fabrication and characterization of microfluidic devices based on boron-modified epoxy resin using CO2 laser ablation for bio-analytical applications, *Sci. Rep.*, 2023, **13**(1), 12623.

91 Effectiveness of front line and emerging fungal disease prevention and control interventions and opportunities to address appropriate eco-sustainable solutions - ScienceDirect, [cited 2024 May 15], available from: https://www.sciencedirect.com/science/article/pii/S0048969722053839.

92 H. Sun, C. W. Chan, Y. Wang, X. Yao, X. Mu and X. Lu, *et al.*, Reliable and reusable whole polypropylene plastic microfluidic devices for a rapid, low-cost antimicrobial susceptibility test, *Lab Chip*, 2019, **19**(17), 2915–2924.

93 G. M. Walker, N. Monteiro-Riviere, J. Rouse and A. T. O'Neill, A linear dilution microfluidic device for cytotoxicity assays, *Lab Chip*, 2007, **7**(2), 226–232.

94 L. Shao, B. Pan, R. Hou, Y. Jin and Y. Yao, User-friendly microfluidic manufacturing of hydrogel microspheres with sharp needle, *Biofabrication*, 2022, **14**(2), 025017.

95 C. W. Tsao, Y. C. Cheng and J. H. Cheng, Fluid Flow Shear Stress Stimulation on a Multiplex Microfluidic Device for Rat Bone Marrow Stromal Cell Differentiation Enhancement, *Micromachines*, 2015, **6**(12), 1996–2009.

96 G. M. Whitesides, The origins and the future of microfluidics, *Nature*, 2006, **442**(7101), 368–373.

97 A. Maurya, J. S. Murallidharan, A. Sharma and A. Agarwal, Microfluidics geometries involved in effective blood plasma separation, *Microfluid. Nanofluid.*, 2022, **26**(10), 73.

98 H. Ashiba, M. Fujimaki, K. Awazu, T. Tanaka and M. Makishima, Microfluidic chips for forward blood typing performed with a multichannel waveguide-mode sensor, *Sens. Biosensin Res.*, 2016, **7**, 121–126.

99 J. Che, E. Sollier, D. E. Go, N. Kummer, M. Rettig and J. Goldman, *et al.*, Microfluidic Vortex Technology For Pure Circulating Tumor Cell Concentration From Patient Blood, in *Proceedings of the 17th International Conference on Miniaturized Systems for Chemistry and Life Sciences (μTAS 2013)*, CBMS, Freiburg, Germany, 2013, pp. 1018–1020.

100 J. N. Sierra Agudelo, F. Subirada, M. Hendriks, R. Rodriguez Trujillo and J. Samitier, Low-cost 3D printed inertial flow microfluidic devices for cellular isolation in liquid biopsies, *Front. Lab Chip Technol.*, 2023, **2**, 1175668.

101 A. J. Mach and D. Di Carlo, Continuous scalable blood filtration device using inertial microfluidics, *Biotechnol. Bioeng.*, 2010, **107**(2), 302–311.

102 C. Macaraniag, J. Zhou, J. Li, W. Putzbach, N. Hay and I. Papautsky, Microfluidic isolation of breast cancer circulating tumor cells from microvolumes of mouse blood, *Electrophoresis*, 2023, **44**(23), 1859–1867.

103 A. Saadat, D. A Huyke, D. I. Oyarzun, P. V. Escobar, I. H. Øvreeide and E. S. G. Shaqfeh, *et al.*, A system for the high-throughput measurement of the shear modulus distribution of human red blood cells, *Lab Chip*, 2020, **20**(16), 2927–2936.

104 B. U. Moon, L. Clime, D. Brassard, A. Boutin, J. Daoud and K. Morton, *et al.*, An automated centrifugal microfluidic assay for whole blood fractionation and isolation of multiple cell populations using an aqueous two-phase system, *Lab Chip*, 2021, **21**(21), 4060–4070.

105 P. M. Aldridge, M. Mukhopadhyay, S. U. Ahmed, W. Zhou, E. Christinck and R. Makonnen, *et al.*, Prismatic Deflection of Live Tumor Cells and Cell Clusters, *ACS Nano*, 2018, **12**(12), 12692–12700.

106 N. Nivedita, N Garg, A. P. Lee and I. Papautsky, A high throughput microfluidic platform for size-selective enrichment of cell populations in tissue and blood samples, *Analyst*, 2017, **142**(14), 2558–2569.

107 M. E. Warkiani, A. K. P. Tay, B. L. Khoo, X. Xiaofeng, J. Han and C. T. Lim, Malaria detection using inertial microfluidics, *Lab Chip*, 2015, **15**(4), 1101–1109.

108 S. Zelenin, J. Hansson, S. Ardabili, H. Ramachandraiah, H. Brismar and A. Russom, Microfluidic-based isolation of bacteria from whole blood for sepsis diagnostics, *Biotechnol. Lett.*, 2015, **37**(4), 825–830.

109 C. Eid and J. G. Santiago, Assay for Listeria monocytogenes cells in whole blood using isotachophoresis and recombinase polymerase amplification, *Analyst*, 2017, **142**(1), 48–54.

110 T. Václavek and F. Foret, Microfluidic device integrating single-cell extraction and electrical lysis for mass spectrometry detection of intracellular compounds, *Electrophoresis*, 2023, **44**(1–2), 313–322.

111 A. Persat, L. A. Marshall and J. G. Santiago, Purification of Nucleic Acids from Whole Blood Using Isotachophoresis, *Anal. Chem.*, 2009, **81**(22), 9507–9511.

112 A. G. Ayers, C. M. Victoriano and S. K. Sia, Integrated device for plasma separation and nucleic acid extraction from whole blood toward point-of-care detection of bloodborne pathogens, *Lab Chip*, 2024, **24**(22), 5124–5136.

113 A. Hatami, M. Saadatmand and M. Garshasbi, Cell-free fetal DNA (cffDNA) extraction from whole blood by using a fully automatic centrifugal microfluidic device based on displacement of magnetic silica beads, *Talanta*, 2024, **267**, 125245.

114 S. Wang, A. Thomas, E. Lee, S. Yang, X. Cheng and Y. Liu, Highly efficient and selective isolation of rare tumor cells

using a microfluidic chip with wavy-herringbone micro-patterned surfaces, *Analyst*, 2016, **141**(7), 2228–22237.

115 D. Z. T. F. Yu, D. K. M. A. Yong and P. J. Fu, Microfluidic Blood Cell Preparation: Now and Beyond, *Small*, 2014, **10**(9), 1687.

116 S. Nagrath, L. V. Sequist, S. Maheswaran, D. W. Bell, D. Irimia and L. Ulkus, *et al.*, Isolation of rare circulating tumour cells in cancer patients by microchip technology, *Nature*, 2007, **450**(7173), 1235–1239.

117 A. Mishra, T. D. Dubash, J. F. Edd, M. K. Jewett, S. G. Garre and N. M. Karabacak, *et al.*, Ultrahigh-throughput magnetic sorting of large blood volumes for epitope-agnostic isolation of circulating tumor cells, *Proc. Natl. Acad. Sci. U. S. A.*, 2020, **117**(29), 16839–16847.

118 J. Alsved, M. Rezayati Charan, P. Ohlsson, A. Urbansky and P. Augustsson, Label-free separation of peripheral blood mononuclear cells from whole blood by gradient acoustic focusing, *Sci. Rep.*, 2024, **14**(1), 8748.

119 H. Torul, Z. Ç. Arslan, T. Tezcan, E. Ç. Kayiş, M. Çalımcı and A. Gumustas, *et al.*, Microfluidic-based blood immunoassays, *J. Pharm. Biomed. Anal.*, 2023, **228**, 115313.

120 J. Kim, J. Yoon, J. Y. Byun, H. Kim, S. Han and J. Kim, *et al.*, Nano-Interstice Driven Powerless Blood Plasma Extraction in a Membrane Filter Integrated Microfluidic Device, *Sensors*, 2021, **21**(4), 1366.

121 M. A. Faridi, H. Ramachandraiah, I. Banerjee, S. Ardabili, S. Zelenin and A. Russom, Elasto-inertial microfluidics for bacteria separation from whole blood for sepsis diagnostics, *J Nanobiotechnol.*, 2017, **15**(1), 3.

122 D. Lee, Y. H. Choi and W. Lee, Enhancement of inflection point focusing and rare-cell separations from untreated whole blood, *Lab Chip*, 2020, **20**(16), 2861–2871.

123 L. Armbrecht, O. Rutschmann, B. M. Szczerba, J. Nikoloff, N. Aceto and P. S. Dittrich, Quantification of Protein Secretion from Circulating Tumor Cells in Microfluidic Chambers, *Adv. Sci.*, 2020, **7**(11), 1903237.

124 R. Jack, K. Hussain, D. Rodrigues, M. Zeinali, E. Azizi and M. Wicha, *et al.*, Microfluidic continuum sorting of sub-populations of tumor cells via surface antibody expression levels, *Lab Chip*, 2017, **17**(7), 1349–1358.

125 E. Ozkumur, A. M. Shah, J. C. Ciciliano, B. L. Emmink, D. T. Miyamoto and E. Brachtel, *et al.*, Inertial Focusing for Tumor Antigen–Dependent and –Independent Sorting of Rare Circulating Tumor Cells, *Sci. Transl. Med.*, 2013, **5**(179), 179ra47.

126 Y. Wang, N. Talukder, B. B. Nunna and E. S. Lee, Dean vortex-enhanced blood plasma separation in self-driven spiral microchannel flow with cross-flow microfilters, *Biomicrofluidics*, 2024, **18**(1), 014104.

127 P. Guevara-Pantoja, Y. Alvarez-Braña, J. Mercader-Ruiz, F. Benito Lopez and L. Basabe-Desmonts, *A Microfluidic Device for Passive Separation of Platelet-Rich Plasma from Whole Blood*, Social Science Research Network, Rochester, NY, 2024 [cited 2025 Apr 16], available from: https://papers.ssrn.com/abstract=5004024.

128 S. C. Gifford, B. C. Strachan, H. Xia, E. Vörös, K. Torabian and T. A. Tomasino, *et al.*, A portable system for processing donated whole blood into high quality components without centrifugation, *PLoS One*, 2018, **13**(1), e0190827.

129 H. Jiang, X. Weng and D. Li, Microfluidic whole-blood immunoassays, *Microfluid. Nanofluid.*, 2011, **10**(5), 941–964.

130 M. Gonçalves, I. M. Gonçalves, J. Borges, V. Faustino, D. Soares and F. Vaz, *et al.*, Polydimethylsiloxane Surface Modification of Microfluidic Devices for Blood Plasma Separation, *Polymers.*, 2024, **16**(10), 1416.

131 S. Srikanth, S. K. Dubey, A. Javed and S. Goel, Droplet based microfluidics integrated with machine learning, *Sens. Actuators, A*, 2021, **332**, 113096.

132 K. Manekar, M. L. Bhaiyya, M. A. Hasamnis and M. B. Kulkarni, Intelligent Microfluidics for Plasma Separation: Integrating Computational Fluid Dynamics and Machine Learning for Optimized Microchannel Design, *Biosensors*, 2025, **15**(2), 94.

133 D. D. Dixit, T. P. Graf, K. J. McHugh and P. B. Lillehoj, Artificial intelligence-enabled microfluidic cytometer using gravity-driven slug flow for rapid CD4+ T cell quantification in whole blood, *Microsyst. Nanoeng.*, 2025, **11**(1), 1–12.

134 V. Rizzuto, A. Mencattini, B. Álvarez-González, D. Di Giuseppe, E. Martinelli and D. Beneitez-Pastor, *et al.*, Combining microfluidics with machine learning algorithms for RBC classification in rare hereditary hemolytic anemia, *Sci. Rep.*, 2021, **11**(1), 13553.

135 U. A. Gurkan, D. K. Wood, D. Carranza, L. H. Herbertson, S. L. Diamond and E. Du, *et al.*, Next generation microfluidics: fulfilling the promise of lab-on-a-chip technologies, *Lab Chip*, 2024, **24**(7), 1867–1874.

136 L. Dean, Blood and the cells it contains, in *Blood Groups and Red Cell Antigens*, National Center for Biotechnology Information (US), 2005, available from: https://www.ncbi.nlm.nih.gov/books/NBK2263/.

137 M. S. Blumenreich, The White Blood Cell and Differential Count, in *Clinical Methods: The History, Physical, and Laboratory Examinations*, ed. H. K. Walker, W. D. Hall and J. W. Hurst, Butterworths, Boston, 3rd edn, 1990, available from: http://www.ncbi.nlm.nih.gov/books/NBK261/.

138 A. Tigner, S. A. Ibrahim and I. V. Murray, *Histology, White Blood Cell*, StatPearls Publishing, Treasure Island (FL), 2024, available from: http://www.ncbi.nlm.nih.gov/books/NBK563148/.

139 S. Majstoravich, J. Zhang, S. Nicholson-Dykstra, S. Linder, W. Friedrich and K. A. Siminovitch, *et al.*, Lymphocyte microvilli are dynamic, actin-dependent structures that do not require Wiskott-Aldrich syndrome protein (WASp) for their morphology, *Blood*, 2004, **104**(5), 1396–1403.

140 Monocyte Count - an overview|ScienceDirect Topics, [cited 2024 Jun 3], available from: https://www.sciencedirect.com/topics/nursing-and-health-professions/monocyte-count.

141 L. Palmer, C. Briggs, S. McFadden, G. Zini, J. Burthem and G. Rozenberg, *et al.*, ICSH recommendations for the standardization of nomenclature and grading of peripheral blood cell morphological features, *Int. J. Lab. Hematol.*, 2015, **37**(3), 287–303.

142 J. Mestas and C. C. W. Hughes, Of Mice and Not Men: Differences between Mouse and Human Immunology, *J. Immunol.*, 2004, **172**(5), 2731–2738.

143 L. M. Kornmann, A. Zernecke, D. M. Curfs, B. J. Janssen, C. Weber and M. P. De Winther, *et al.*, Echogenic perfluorohexane-loaded macrophages adhere in vivo to activated vascular endothelium in mice, an explorative study, *Cardiovasc. Ultrasound*, 2015, **13**(1), 1.

144 Cleveland Clinic, [cited 2024 Jun 3], Basophilia: Definition, Causes, Symptoms & Treatment, available from: **https://my.clevelandclinic.org/health/diseases/22099-basophilia**.

145 Blood Differential: MedlinePlus Medical Test, [cited 2024 May 5], available from: **https://medlineplus.gov/lab-tests/blood-differential/**.

146 T. G. Uhm, B. S. Kim and I. Y. Chung, Eosinophil Development, Regulation of Eosinophil-Specific Genes, and Role of Eosinophils in the Pathogenesis of Asthma, *Allergy, Asthma Immunol. Res.*, 2012, **4**(2), 68–79.

147 J. J. Lee, E. A. Jacobsen, S. I. Ochkur, M. P. McGarry, R. M. Condjella and A. D. Doyle, *et al.*, Human vs. Mouse Eosinophils: That which we call an eosinophil, by any other name would stain as red, *J. Allergy Clin. Immunol.*, 2012, **130**(3), 572–584.

148 W. B. Mitchell, Platelets, in *Reference Module in Biomedical Sciences*, Elsevier, 2014, available from: **https://www.sciencedirect.com/science/article/pii/B9780128012383000623**.

149 M. Jirouskova, A. S. Shet and G. J. Johnson, A guide to murine platelet structure, function, assays, and genetic alterations, *J. Thromb. Haemostasis*, 2007, **5**(4), 661–669.

150 J. H. Im and R. J. Muschel, Protocol for Murine/Mouse Platelets Isolation and Their Reintroduction in vivo, *Bio-Protoc.*, 2017, **7**(4), e2132.

151 A. D. Sung, R. C. Yen, Y. Jiao, A. Bernanke, D. A. Lewis and S. E. Miller, *et al.*, Fibrinogen-Coated Albumin Nanospheres Prevent Thrombocytopenia-Related Bleeding, *Radiat. Res.*, 2020, **194**(2), 162–172.

152 P. E. Vandeventer, K. M. Weigel, J. Salazar, B. Erwin, B. Irvine and R. Doebler, *et al.*, Mechanical Disruption of Lysis-Resistant Bacterial Cells by Use of a Miniature, Low-Power, Disposable Device, *J. Clin. Microbiol.*, 2011, **49**(7), 2533–2539.

153 I. Sovadinova, E. F. Palermo, R. Huang, L. M. Thoma and K. Kuroda, Mechanism of Polymer-Induced Hemolysis: Nanosized Pore Formation and Osmotic Lysis, *Biomacromolecules*, 2011, **12**(1), 260–268.

154 X. Y. Wei, J. H. Li, L. Wang and F. Yang, Low-voltage electrical cell lysis using a microfluidic device, *Biomed. Microdevices*, 2019, **21**(1), 22.

155 M. S. Islam, A. Shahid, K. Kuryllo, Y. Li, M. J. Deen and P. R. Selvaganapathy, Electrophoretic Concentration and Electrical Lysis of Bacteria in a Microfluidic Device Using a Nanoporous Membrane, *Micromachines*, 2017, **8**(2), 45.